Glycobiology Advance Access published June 19, 2013

Glycobiology vol. 0 no. 0 pp. 1–17, 2013
doi:10.1093/glycob/cwt028

O-GlcNAc transferase inhibits KSHV propagation and modifies replication relevant viral proteins as detected by systematic O-GlcNAcylation analysis

Ramona Jochmann[2], Jens Pfannstiel[3], Priya Chudasama[2], Elisabeth Kuhn[2], Andreas Konrad[2], and Michael Stürzl[1,2]

[2]Division of Molecular and Experimental Surgery, University Medical Center Erlangen, Friedrich-Alexander University of Erlangen-Nuremberg, Schwabachanlage 10, 91054 Erlangen, Germany and [3]Core Facility of the Life Science Center of the University Hohenheim, August von Hartmann Str. 3, 70599 Stuttgart, Germany

Received on July 20, 2012; revised on March 21, 2013; accepted on April 4, 2013

O-GlcNAcylation is an inducible, highly dynamic and reversible post-translational modification, mediated by a unique enzyme named *O*-linked *N*-acetyl-D-glucosamine (*O*-GlcNAc) transferase (OGT). In response to nutrients, *O*-GlcNAc levels are differentially regulated on many cellular proteins involved in gene expression, translation, immune reactions, protein degradation, protein–protein interaction, apoptosis and signal transduction. In contrast to eukaryotic cells, little is known about the role of O-GlcNAcylation in the viral life cycle. Here, we show that the overexpression of the OGT reduces the replication efficiency of Kaposi's sarcoma-associated herpesvirus (KSHV) in a dose-dependent manner. In order to investigate the global impact of O-GlcNAcylation in the KSHV life cycle, we systematically analyzed the 85 annotated KSHV-encoded open reading frames for *O*-GlcNAc modification. For this purpose, an immunoprecipitation (IP) strategy with three different approaches was carried out and the *O*-GlcNAc signal of the identified proteins was properly controlled for specificity. Out of the 85 KSHV-encoded proteins, 18 proteins were found to be direct targets for O-GlcNAcylation. Selected proteins were further confirmed by mass spectrometry for *O*-GlcNAc modification. Correlation of the functional annotation and the *O*-GlcNAc status of KSHV proteins showed that the predominant targets were proteins involved in viral DNA synthesis and replication. These results indicate that O-GlcNAcylation plays a major role in the regulation of KSHV propagation.

Keywords: DNA replication / DNA synthesis / Kaposi's sarcoma / KSHV / *O*-GlcNAc

[1]To whom correspondence should be addressed: Tel: +49-9131-85 33109; Fax: +49-9131-85 32077; e-mail: michael.stuerzl@uk-erlangen.de

Introduction

In eukaryotic cells, a myriad of cytoplasmic, nuclear, and mitochondrial proteins are post-translationally modified by the O-linkage of the monosaccharide *N*-acetyl-D-glucosamine (*O*-GlcNAc) to serine and threonine residues (Hart 1997; Zachara and Hart 2006). O-GlcNAcylation is a highly dynamic and reversible post-translational modification, which differs from other glycosylation events in that it occurs in the cytosol and the nucleus rather than in the Golgi apparatus or the endoplasmic reticulum. The addition and removal of *O*-GlcNAc is catalyzed by two unique enzymes called *O*-GlcNAc transferase (OGT) and *O*-GlcNAc hexosaminidase (OGA; Iyer and Hart 2003).

Most of the proteins that have been described to be O-GlcNAcylated are phosphoproteins, and an extensive interplay between O-GlcNAcylation and serine/threonine phosphorylation in a variety of proteins has been reported to exist (Butkinaree et al. 2010; Wang et al. 2010; Wang, Huang, et al. 2012). Moreover, several proteins, including c-myc, estrogen receptors, Sp1 and RNA polymerase II (RNA pol-II), exhibit a global as well as site-specific reciprocal relationship between *O*-GlcNAc and O-phosphate in response to stimuli (Kamemura and Hart 2003; Slawson and Hart 2003). This indicates that, in some cases, O-GlcNAcylation can act as an antagonist for protein phosphorylation (Chou et al. 1995; Cole and Hart 1999; Cheng et al. 2000; Cheng and Hart 2001; Comer and Hart 2001; Kamemura and Hart 2003). O-GlcNAcylation and phosphorylation share many similarities: both take place in the nucleus and cytoplasm, occur in a dynamic manner in response to external stimuli and modulate protein functions by controlling enzyme activity, protein–protein interactions, subcellular localization and transactivation potential (Zachara and Hart 2004; Love and Hanover 2005). The dynamic nature of O-GlcNAcylation and its interplay with phosphorylation has thus attracted the interest of cell signaling research on *O*-GlcNAc modification.

In nearly 30 years of *O*-GlcNAc research, it has been shown that *O*-GlcNAc regulates cellular processes such as gene expression, proteasomal degradation and signaling. Increasing evidence suggests that the main function of *O*-GlcNAc is the regulation of gene expression. First of all, the carboxy-terminal domain (CTD) of the RNA pol-II is abundantly O-GlcNAcylated (Kelly et al. 1993). Interestingly, transcriptionally active RNA pol-II is not O-GlcNAcylated, but extensively phosphorylated at the CTD, suggesting that *O*-GlcNAc

associates with the transcriptionally inactive form and is involved in the initiation of transcription (Comer and Hart 2001; Ranuncolo et al. 2012). Second, virtually every RNA pol-II-associated transcription factor analyzed to date has been found to be modified by *O*-GlcNAc, including constitutively active transcription factors such as Sp1 (Jackson and Tjian 1988; Roos et al. 1997) as well as tightly regulated transcription factors such as c-myc and NF-κB (Chou et al. 1995; Golks et al. 2007). Third, *O*-GlcNAc is further associated with transcriptional repressors, such as mSin3A (Yang et al. 2002), and the polycomb group (Love et al. 2010), indicating that *O*-GlcNAc plays an essential role in the repression of gene expression.

Although much progress has been made on deciphering the role of *O*-GlcNAc in cellular regulation, little is known about the impact of *O*-GlcNAc in the regulation of the viral life cycle. We have previously described that *O*-GlcNAc regulates the propagation of the human immunodeficiency virus type-1 (HIV-1). Increased O-GlcNAcylation of the cellular transcription factor Sp1 resulted in an inhibition of the HIV-1 promoter (Jochmann et al. 2009). Moreover, *O*-GlcNAc modifications have been demonstrated on few viral proteins, such as the large T antigen of the Simian virus-40 (Medina et al. 1998), the major tegument protein UL32 of the human cytomegalovirus (Novelli and Boulanger 1991; Greis et al. 1994), the tegument protein gp41 of the baculovirus (Whitford and Faulkner 1992), the fiber protein of adenovirus types 2 and 5 (Mullis et al. 1990) as well as on the non-structural rotavirus NS26 protein (Gonzalez and Burrone 1991). However, the function of *O*-GlcNAc on any of these proteins is not yet known. Just recently, an additional protein was added to the list, namely the gene product of the open reading frame (ORF) 50, the viral replication and transcription activator (RTA) of the Kaposi's sarcoma-associated herpesvirus (KSHV; Ko et al. 2012). In this work, Ko et al. found that O-GlcNAcylation of ORF50 reduces its transactivation potential, mainly due to the enhanced interaction of ORF50 with its negative regulator poly-ADP ribose polymerase-1, thereby leading to suppressed viral replication.

KSHV, also known as human herpesvirus type-8, was originally identified in 1994 in Kaposi's sarcoma (KS) lesions (Chang et al. 1994) and is regarded as the etiologic agent of KS. KSHV encodes 85 different ORFs (Glenn et al. 1999), which follow an ordered sequence of expression upon the activation of lytic replication. The aim of this study was to determine the effect of OGT on the viral replication and on the global O-GlcNAcylation of all KSHV-encoded proteins. We found that the overexpression of OGT in KSHV-infected human embryonic kidney 293 (HEK293) cells reduces the viral replication efficiency in a dose-dependent manner. By systematically investigating all the KSHV-encoded proteins, we found 18 proteins to be modified by *O*-GlcNAc; the majority of these proteins are known to regulate viral DNA synthesis and replication. These results strongly indicate that the *O*-GlcNAc modification of viral proteins may play an important role in the regulation of KSHV propagation.

Results

OGT blocks KSHV propagation

To investigate the effect of *O*-GlcNAc on viral propagation, KSHV-infected (rKSHV.219) HEK293 cells were used as a model system. The viral strain rKSHV.219 is a recombinant KSHV that constitutively expresses the green fluorescent protein (GFP) under the control of the EF1α promoter (Vieira and O'Hearn 2004). Thus, cells infected with rKSHV.219 are easily detectable by GFP fluorescence. KSHV-infected HEK293 cells (producer cells) were transfected with increasing amounts of a plasmid encoding OGT and lytic replication was induced either by treatment with 3 mM sodium butyrate (NaBu) or by co-transfection with the viral trans-activator ORF50 (Figure 1A, upper panel). Virus-containing supernatants were collected and used to newly infect HEK293 cells (indicator cells), while the producer cells were lysed and subsequently subjected to western blot analysis. Increasing expression of OGT as well as increasing *O*-GlcNAc levels in the

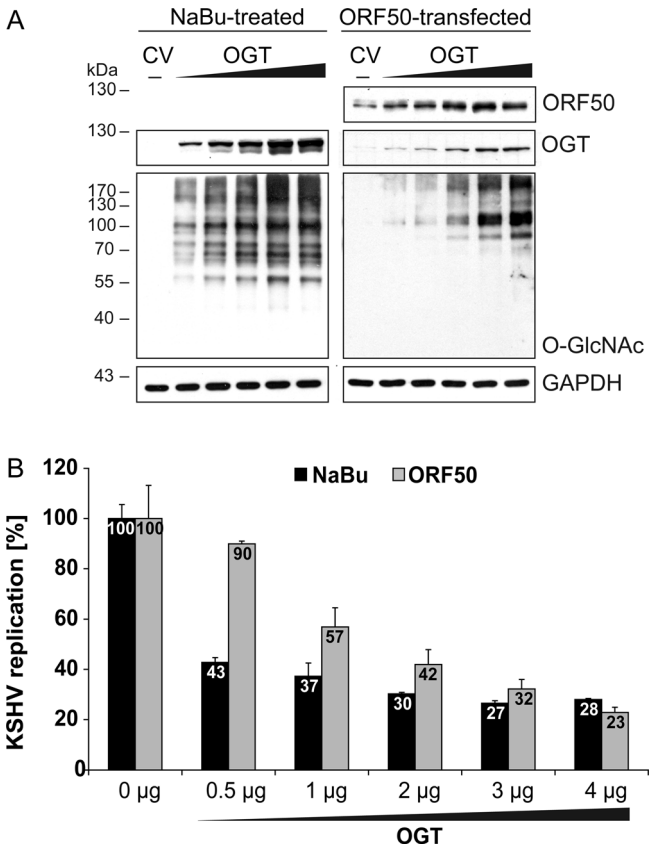

Fig. 1. Overexpression of OGT in KSHV-infected HEK293 cells reduces viral replication. (**A**) HEK293-rKSHV.219 cells (producer cells) were transiently transfected either with control vector (CV) or with increasing amounts of a plasmid encoding OGT. The total DNA amount was adjusted to the same content with CV. The cells were either treated with 3 mM NaBu or co-transfected with ORF50 to induce the lytic KSHV replication. The expression of OGT and ORF50, as well as the *O*-GlcNAc level were monitored by western blot; GAPDH served as a loading control. (**B**) The cell culture supernatants from (A) were collected and cell debris was removed by centrifugation twice at 500 × *g* for 5 min. HEK293 cells (indicator cells) were cultured with the supernatants for 24 h prior to media change. After cultivation for an additional 2 days, the amount of KSHV-infected cells (GFP-positive) was determined by flow cytometry. For each sample, 1×10^5 cells were counted. The number of KSHV-infected cells cultured with supernatant from CV-transfected cells was defined as 100%. One representative out of three independent experiments is shown.

producer cells could be confirmed (Figure 1A, middle panels). Equal loading was monitored by glyceraldehyde 3-phosphate dehydrogenase (GAPDH) staining (Figure 1A, lower panels). Flow cytometric evaluation of indicator cells showed that OGT decreased KSHV infectivity in a dose-dependent manner (Figure 1B), independently of whether the lytic replication was induced by NaBu treatment (Figure 1B, black bars) or by co-transfection with ORF50 (Figure 1B, gray bars).

In order to determine whether the reduced KSHV infectivity was specifically due to increased O-GlcNAcylation, two approaches were followed. First, ectopically expressed OGT was knocked down by RNA interference (Figure 2A–C). The specificity of the siRNA was verified with an OGT rescue mutant (rOGT)-encoding plasmid, which contains six silent nucleotide exchanges in the siRNA-binding site (Jochmann et al. 2009). Lytic KSHV replication was induced by treatment with 3 mM NaBu. Western blot analysis proved that the overexpression of OGT was significantly depleted in HEK293-rKSHV.219 cells co-transfected with the OGT-targeting siRNA (Figure 2A, top panel, lanes 2 and 3), whereas the expression of rOGT was not affected (Figure 2A, top panel, lane 4). Staining of O-GlcNAcylated proteins in the producer cells confirmed the catalytic activity of OGT and rOGT (Figure 2A, middle panel), whereas GAPDH staining confirmed the loading of equal protein amounts (Figure 2A, bottom panel). Three days after the induction of lytic replication, virus-containing supernatants were collected. To rule out any cytotoxic effects upon the overexpression of OGT, the number of viable producer cells was determined by cell counting (Figure 2B); no decrease in the cell viability and survival was observed upon the overexpression of OGT. In contrast, a trend was visible, which indicated that cells overexpressing OGT exhibited increased cell survival upon the induction of lytic replication, whereas the knockdown of OGT overexpression to nearly endogenous levels decreased the cell survival to that of the control (Figure 2B). The infectivity of supernatants collected from these cells was determined by the new infection of HEK293 indicator cells and subsequent flow cytometric evaluation. The overexpression of OGT decreased KSHV infectivity, whereas the knockdown of OGT restored the production of viral particles (Figure 2C). In contrast, rOGT escaped silencing and was still able to suppress KSHV infectivity in the presence of OGT siRNA (Figure 2C).

The second approach made use of Thiamet G, a chemical inhibitor of OGA activity (Figure 2D–F). Treatment of lytically replicating producer cells with increasing concentrations of Thiamet G resulted in an increase in the overall *O*-GlcNAc level (Figure 2D). To exclude any cytotoxic effects upon treatment with Thiamet G, the number of viable producer cells was determined by cell counting. As for OGT overexpression, no decrease but a slight dose-dependent increase in the cell number was observed according to the Thiamet G concentration (Figure 2E). Subsequently, the KSHV replication efficiency was assessed in the indicator cells by flow cytometry (Figure 2F). A significant dose-dependent decrease in the KSHV replication efficiency was observed according to the Thiamet G concentration. Of note, Thiamet G inhibited KSHV replication in low concentrations (Figure 2F, 1 nM), whereas it had no significant impact on the cell number in 100-fold higher concentrations (Figure 2E, 100 nM). This indicates that the inhibitory effect of OGT on KSHV replication is not due to the effects of Thiamet G on cell proliferation and/or cell death.

Identification of the O-*GlcNAc proteome of KSHV*

The stimuli which trigger the initiation of lytic KSHV replication are still insufficiently understood. The molecular switch for the initiation of the lytic gene expression program is ORF50, which alone is necessary and sufficient to induce the lytic replication. In a previous study, it was shown that ORF50 is modified with *O*-GlcNAc and that this modification suppresses its activity (Ko et al. 2012). To determine whether O-GlcNAcylation also affects other viral processes, we systematically analyzed the 85 annotated KSHV-encoded proteins for *O*-GlcNAc modification. For the investigation of the complete KSHV proteome, we developed a tripartite immunoprecipitation (IP) workflow (Figure 3). To ensure the efficient O-GlcNAcylation of all putative viral proteins, HEK293T cells were transfected with expression plasmids for the individual KSHV protein together with an expression plasmid for OGT. As all of the individual KSHV proteins are myc-tagged (Sander et al. 2008; Konrad et al. 2009), expression of the transfected KSHV-encoded proteins was controlled by western blot using an anti-myc antibody (Supplementary data, Figure S1). Out of the 85 KSHV-encoded proteins, 5 were undetectable by western blot (Supplementary data, Figure S1 and Table I, column 2); the remaining 80 proteins were subjected to further investigations.

First, IP was performed using the anti-*O*-GlcNAc antibody CTD110.6 coupled to cyanogen bromide-activated agarose (Figure 3A). The enrichment of KSHV-encoded proteins was verified by western blot staining with an anti-myc antibody. Out of the 80 expressed KSHV proteins, 59 proteins were enriched by *O*-GlcNAc IP (Supplementary data, Figure S2 and Table I, column 3). However, using this method, not only may O-GlcNAcylated proteins be enriched, but also proteins that interact with O-GlcNAcylated proteins. In order to rule out the co-precipitation of unmodified KSHV-encoded proteins, IP was repeated using magnetic beads coupled to an anti-myc antibody (Figure 3B); this approach specifically precipitates KSHV-encoded proteins. The efficiency of the IP was analyzed by western blot with an anti-myc antibody (data not shown). Subsequently, the precipitated proteins were stained with the anti-*O*-GlcNAc antibody. In this approach, 23 proteins were found to be O-GlcNAcylated, whereas 57 proteins did not show any *O*-GlcNAc staining (Supplementary data, Figure S3 and Table I, column 4). Of note, the determination of the *O*-GlcNAc status of some proteins was hampered by the co-migration of heavy or light chains of the immunoglobulin (ORF10, ORF11, ORF18, ORF23, ORF31, ORF32, ORF36 and ORF K9).

For further analyses, only those proteins with positive *O*-GlcNAc status in both procedures were regarded as true candidates that were potentially modified by *O*-GlcNAc. In total, there were 20 proteins that were considered candidates: ORF8, ORF9, ORF2, ORF K3, ORF17, ORF21, ORF25, ORF29, ORF44, ORF K8, ORF54, ORF K10, ORF K10.5, ORF

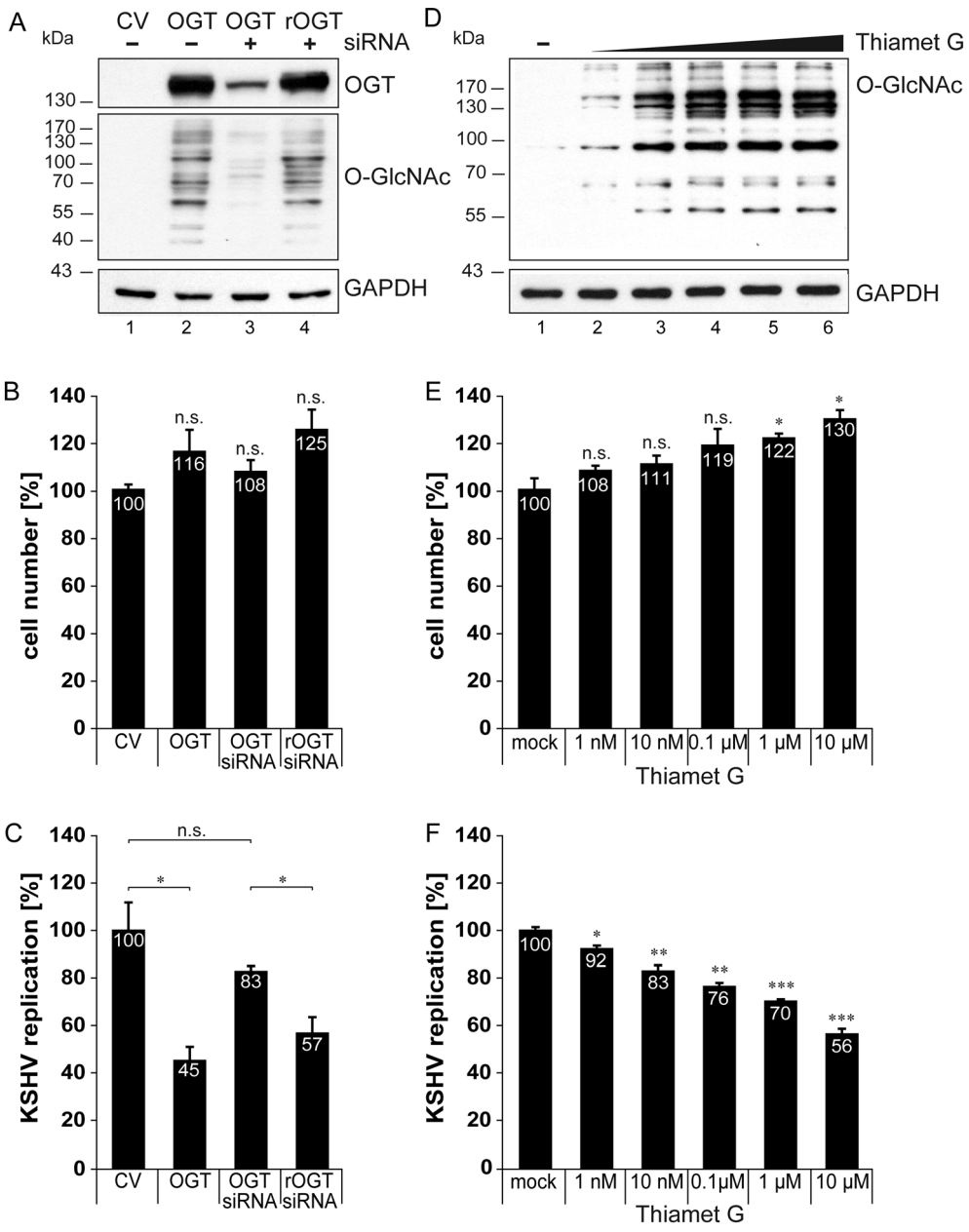

Fig. 2. Increased O-GlcNAcylation in KSHV-infected HEK293 cells reduces viral replication. (**A**–**C**) HEK293-rKSHV.219 cells (producer cells) were transfected with control vector (CV) or with plasmids encoding either OGT or the rOGT containing six silent mutations in the siRNA binding site, along with an siRNA depleting OGT. The cells were treated with 3 mM NaBu in order to induce the lytic replication of KSHV. Similarly, HEK293-rKSHV.219 producer cells were treated with increasing concentrations of Thiamet G prior to the induction of lytic replication with NaBu (**D**–**F**). Three days post-treatment, virus-containing supernatants were collected, while the still-attached cells were harvested and counted using a cell counter (B and E). Subsequently, cells were lysed in RIPA buffer and subjected to western blot (A and D) to monitor *O*-GlcNAc levels and the expression profile of OGT. Staining of GAPDH served as a loading control. HEK293 cells (indicator cells) were cultured with the collected supernatants. The amount of newly infected cells was determined by flow cytometry three days post-infection (C and F). For each sample, 1×10^5 cells were counted. The number of KSHV-infected cells cultured either with supernatant from CV-transfected cells (C) or with supernatant from only NaBu-treated cells (F) was defined as 100%.The mean ± SD calculated from triplicate determinations are indicated. The *P*-values are given for comparison with control: n.s., not significant; $*P \leq 0.05$; $**P \leq 0.01$; $***P \leq 0.001$. One representative out of three independent experiments is shown.

K11, ORF59, ORF60, ORF61, ORF63, ORF69 and ORF75. In order to confirm these data, the 20 identified proteins were subjected to a third additional IP using an anti-myc antibody covalently coupled to agarose beads (Figure 3C). The efficiency of the IP was evaluated by staining with the anti-myc antibody (Figure 4, upper panels). The *O*-GlcNAc modification of all proteins could be confirmed (Figure 4, asterisks in lower panels and Table I, column 5). Thus, a total of 20 proteins were reproducibly identified to be *O*-GlcNAc modified using three different IP procedures.

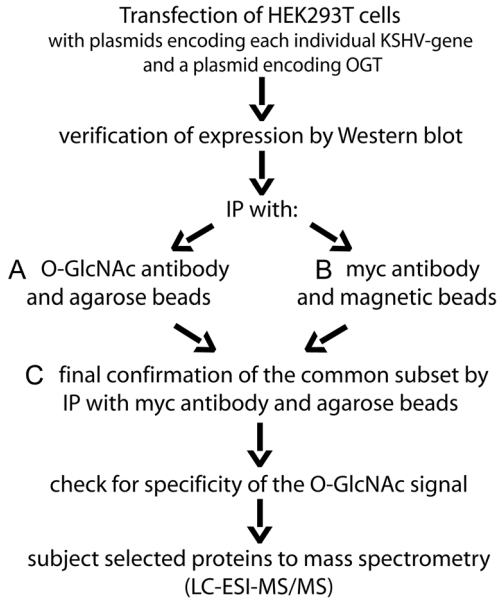

Fig. 3. Workflow of the determination of O-GlcNAcylated proteins in the KSHV proteome. HEK293T cells were transfected with OGT and with plasmids encoding the individual KSHV genes. Cells were lysed and the expression was verified by western blot using an anti-myc antibody. (**A**) The lysates were subjected to IP using the anti-*O*-GlcNAc antibody (CTD110.6) and anti-IgM-coupled cyanogen bromide-activated agarose beads. Precipitates were counterstained in western blot analysis using an anti-myc antibody. (**B**) IPs were performed using an anti-myc antibody coupled to magnetic beads. Western blot staining was performed using an anti-*O*-GlcNAc antibody. (**C**) From the proteins identified to be O-GlcNAcylated in (A) and (B), IPs were performed with an anti-myc antibody covalently coupled to agarose beads. Precipitates were counterstained in western blot analysis using an anti-*O*-GlcNAc antibody. The *O*-GlcNAc signal on the identified candidates was checked for specificity by PNGase F digest and by competition with free GlcNAc. Six proteins were selected for further investigations by MS: the IP eluates were separated on a gel, excised and subjected to LC-ESI-MS/MS.

Specificity of O-*GlcNAc modification on the identified proteins*

The *O*-GlcNAc antibody used in this study (monoclonal anti-*O*-GlcNAc antibody, clone CTD110.6) has recently been demonstrated to cross-react with some *N*-linked glycans (Isono 2011). To rule out any false positives, all putative *O*-GlcNAc-modified proteins (IP eluate) were treated with PNGase F [peptide-*N*(4)-(*N*-acetyl-β-D-glucosaminyl)asparagine amidase F], which is an enzyme that cleaves *N*-linked glycoproteins between the innermost GlcNAc and asparagine residues. The detection of a decreased CTD110.6 signal together with a shift of the signal towards a lower molecular weight would indicate false-positive *O*-GlcNAc staining. As a positive control for the removal of *N*-glycans by PNGase F, recombinant ovalbumin was treated with PNGase F (P) or left untreated (mock, M), followed by silver staining to monitor equal loading (Figure 5A, left panel). Staining with the fluorescein isothiocyanate (FITC)-labeled lectin Concanavalin A (ConA-FITC) served to assess changes in N-glycosylation. PNGase F treatment markedly reduced the ConA staining and the molecular weight of ovalbumin (Figure 5A). The same procedure was applied to the 20 KSHV proteins that were assumed

Table I. O-GlcNAcylation of KSHV-encoded proteins

Gene/protein	Expression	Myc detection after *O*-GlcNAc IP (agarose beads)	*O*-GlcNAc detection after myc-IP (magnetic beads)	*O*-GlcNAc detection after myc-IP (agarose beads)	Specificity of *O*-GlcNAc signal confirmed
ORF K1	+	+	n.d.		
ORF4	+	n.d.	n.d.		
ORF6	+	+	n.d.		
ORF7	+	n.d.	n.d.		
ORF8	+	+	+	+	+
ORF9	+	+	+	+	+
ORF10	+	+	n.d.		
ORF11	+	+	n.d.		
ORF K2	+	+	n.d.		
ORF2	+	+	+	+	+
ORF K3	+	+	+	+	+
ORF70	+	+	n.d.		
ORF K4	+	+	n.d.		
ORF K4.1	+	n.d.	n.d.		
ORF K4.2	+	+	n.d.		
ORF K5	+	+	n.d.		
ORF K6	+	n.d.	n.d.		
ORF K7	+	n.d.	n.d.		
ORF16	+	+	n.d.		
ORF17	+	+	+	+	+
ORF18	+	+	n.d.		
ORF19	+	+	n.d.		
ORF20	+	+	n.d.		
ORF21	+	+	+	+	+
ORF22	+	n.d.	+		
ORF23	+	+	n.d.		
ORF24	+	n.d.	n.d.		
ORF25	+	+	+	+	+
ORF26	+	+	n.d.		
ORF27	+	+	n.d.		
ORF28	+	+	n.d.		
ORF29	+	+	+	+	+
ORF31	+	+	n.d.		
ORF32	+	n.d.	n.d.		
ORF33	+	+	n.d.		
ORF34	+	n.d.	n.d.		
ORF35	+	+	n.d.		
ORF36	+	+	n.d.		
ORF37	+	+	n.d.		
ORF38	+	n.d.	+		
ORF40/41	+	+	n.d.		
ORF42	+	n.d.	n.d.		
ORF43	+	n.d.	n.d.		
ORF44	+	+	+	+	+
ORF45	+	+	n.d.		
ORF46	+	+	n.d.		
ORF47	+	+	n.d.		
ORF48	+	+	n.d.		
ORF49	+	+	n.d.		
ORF50	+	+ (ORF50)	n.d.		
ORF K8	+	+	+	+	+
ORF K8.1 beta	+	n.d.	n.d.		
ORF52	+	n.d.	n.d.		
ORF53	+	n.d.	n.d.		
ORF54	+	+	+	+	+
ORF55	+	+	n.d.		
ORF56	+	+	n.d.		
ORF K9	+	+	n.d.		
ORF K10	+	+	+	+	+
ORF K10.5	+	+	+	+	no
ORF K11	+	+	+	+	+
ORF59	+	+	+	+	no
ORF60	+	+	+	+	+
ORF61	+	+	+	+	+
ORF62	+	+	n.d.		
ORF63	+	+	+	+	+
ORF64	+	n.d.	+		
ORF66	+	+	n.d.		
ORF67	+	+	n.d.		
ORF67.5	+	n.d.	n.d.		
ORF68	+	+	n.d.		
ORF69	+	+	+	+	+

Continued

Table I. (Continued)

Gene/protein	Expression	Myc detection after *O*-GlcNAc IP (agarose beads)	*O*-GlcNAc detection after myc-IP (magnetic beads)	*O*-GlcNAc detection after myc-IP (agarose beads)	Specificity of *O*-GlcNAc signal confirmed
ORF K12	+	n.d.	n.d.		
ORF K13	+	n.d.	n.d.		
ORF72	+	+	n.d.		
ORF73	+	+ (ORF73)	n.d.		
ORF K14	+	n.d.	n.d.		
ORF74	+	n.d.	n.d.		
ORF75	+	+	+	+	+
ORF K15	+	+	n.d.		
ORF30	n.d. in WB	n.a.	n.a.	n.a.	n.a.
ORF39	n.d. in WB	n.a.	n.a.	n.a.	n.a.
ORF57	n.d. in WB	n.a.	n.a.	n.a.	n.a.
ORF58	n.d. in WB	n.a.	n.a.	n.a.	n.a.
ORF65	n.d. in WB	n.a.	n.a.	n.a.	n.a.

+, positive; n.a., not available; n.d., not determinable. ORF50 and ORF73 were detected to be O-GlcNAcylated by IP with the anti-*O*-GlcNAc antibody and staining with the respective antibody (anti-ORF50 or anti-ORF73 antibody), as indicated in column 3 in brackets.

to be *O*-GlcNAcylated. From those proteins, only ORF8 seemed to be modified by *N*-linked glycans, as the *O*-GlcNAc signal shifts to a lower molecular weight protein upon PNGase F treatment (Figure 5B, ORF8). However, it seems that both modifications (*N*- and *O*-GlcNAc) occur on ORF8 simultaneously, as the *O*-GlcNAc signal on ORF8 was still visible after PNGase F digest. All other proteins were not affected by the PNGase F digest, indicating that they were not modified with *N*-linked glycans under the chosen conditions. In addition, all western blots utilizing CTD 110.6 were controlled by blocking the signal with free GlcNAc (Figure 5, α-*O*-GlcNAc + competition). Hereby, it became clear that ORF59 and ORF K10.5 were non-specifically detected by the anti-*O*-GlcNAc antibody, as the signal was not reduced in the presence of free GlcNAc. Thus, a total of 18 KSHV proteins were found to be specifically *O*-GlcNAc-modified in this study: ORF8, ORF9, ORF2, ORF K3, ORF17, ORF21, ORF25, ORF29, ORF44, ORF K8, ORF54, ORF K10, ORF K11, ORF60, ORF61, ORF63, ORF69 and ORF75 (summarized in Table I).

ORF75 is also O-GlcNAcylated in infected cells

As yet, the O-GlcNAcylation status of these proteins has been assessed exclusively with recombinantly expressed proteins. To prove the validity of this technique, we demonstrated that the viral tegument protein ORF75 is also *O*-GlcNAc modified in infected cells during the lytic replication cycle. As a model system, iSLK-RTA-KSHV.219 cells infected with the recombinant KSHV strain rKSHV.219 were used; these cells are stably transfected with ORF50. Induction of ORF50 expression (by doxycycline treatment) starts the lytic replication cycle and the expression of ORF75 (Figure 6, upper panel). The IP of ORF75 was performed by using a specifically generated anti-ORF75 antibody coupled to Protein A/G-Sepharose (Figure 6, middle panel). Virus-encoded ORF75 was *O*-GlcNAc modified in infected cells (Figure 6, lower panel), confirming the reliability of the employed methods.

Evaluation of O-*GlcNAc-modified proteins by mass spectrometry*

To further validate these data, the *O*-GlcNAc modification of selected proteins was further analyzed by mass spectrometry (MS). To this goal, proteins were selected which were either strongly (ORF K3, ORF K10), moderately (ORF K8, ORF44) or weakly (ORF21, ORF29) O-GlcNAcylated (Figure 4 and Table II). Enriched fractions from IP with an anti-myc agarose were separated by sodium dodecyl sulfate–polyacrylamide gel electrophoresis (SDS–PAGE) and visualized by Coomassie staining (Figure 7A). The precipitated KSHV-encoded proteins were excised from the gel, digested with trypsin or chymotrypsin and investigated by nano liquid chromatography–electrospray ionization tandem mass spectrometry (nano-LC-ESI-MS/MS) on a linear trap quadrupole (LTQ)-Orbitrap XL. Proteins and *O*-GlcNAc-modified peptides were identified by database searches against the NCBI protein sequence database using the Mascot algorithm. The total sequence coverage of the analyzed proteins was between 37 and 75% (Table II); several peptides containing an *O*-GlcNAc site were revealed (Table II and Supplementary data, Figure S4). One selected peptide of ORF K10 containing the *O*-GlcNAc modification of threonine at position 632 is illustrated (Figure 7B). The signal intensity of the IP analyses corresponded well to the number of identified *O*-GlcNAc sites for each protein (Table II), which also

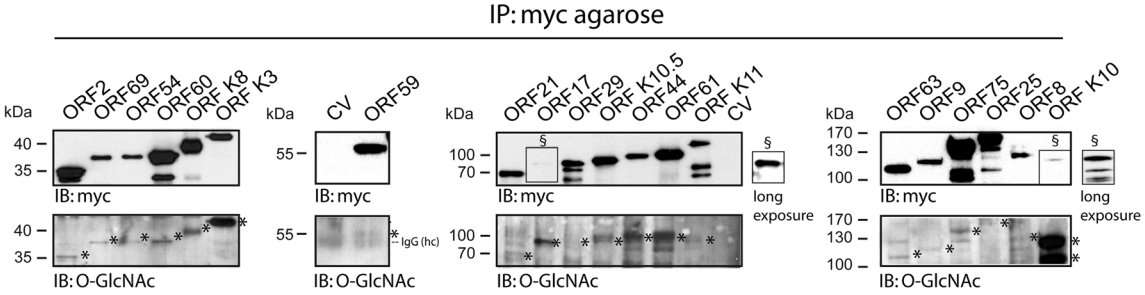

Fig. 4. *O*-GlcNAc detection on KSHV-encoded proteins by IP. Lysates from HEK293T cells transfected with plasmids encoding the designated proteins were subjected to IP using agarose beads covalently coupled to the anti-myc antibody. The precipitates were stained with an anti-myc antibody to control IP efficiency (upper panels) or stained with the anti-*O*-GlcNAc CTD110.6 antibody to analyze O-GlcNAcylation (lower panels). The asterisk indicates the band of O-GlcNAcylated protein; § indicates longer exposure. CV, control vector; IgG(hc), immunoglobulin heavy chain.

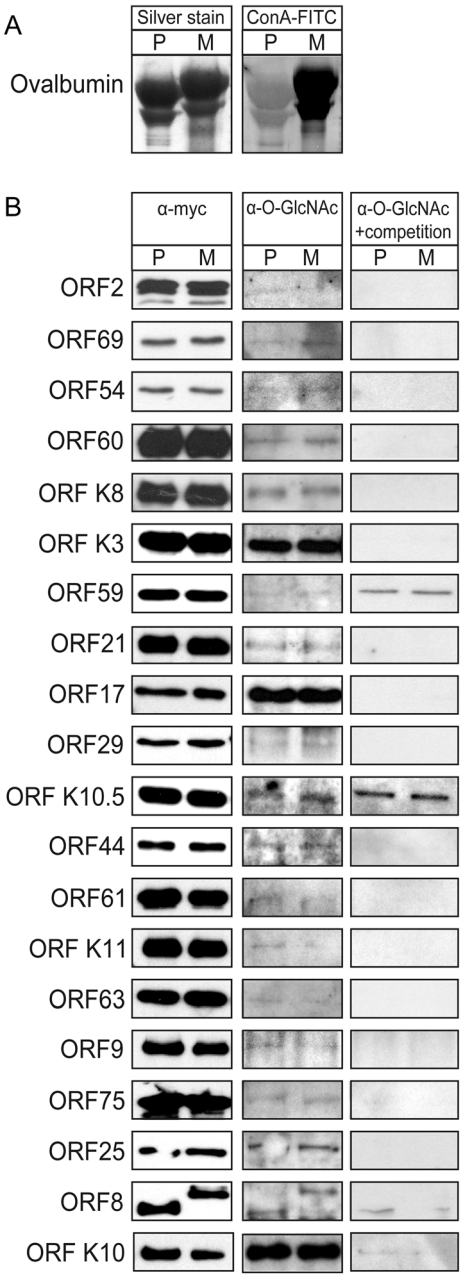

Fig. 5. Specificity controls reveal a total of 18 *O*-GlcNAc-modified KSHV proteins. (**A**) As a proof of principle, recombinant ovalbumin was subjected to PNGase F digest (P) or mock treatment (M). Silver staining indicates equal loading of the recombinant protein. Western blot staining with ConA-FITC indicates removal of *N*-glycans upon PNGase F treatment. (**B**) IP eluates of the potentially *O*-GlcNAc-modified KSHV proteins were subjected to PNGase F digest (P) or mock treatment (M). Western blot staining with the anti-myc antibody indicates IP efficiency. Staining with an anti-*O*-GlcNAc antibody indicates O-GlcNAcylation. Competition with free GlcNAc served as a specificity control for the *O*-GlcNAc signal.

confirmed the stringency and specificity of the IP data. For each identified protein, the Mascot score, the sequence coverage and the number of *O*-GlcNAc peptides identified are given in Table II.

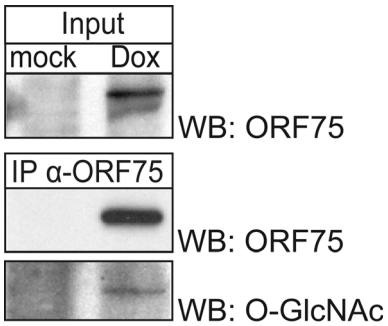

Fig. 6. Virus-encoded ORF75 is *O*-GlcNAc modified in infected cells. Doxycyclin-treated iSLK-RTA-KSHV.219 (1 μg/mL Dox for 4 days) were subjected to IP with an anti-ORF75 antibody and Protein A/G sepharose. The input indicates the expression of ORF75 upon induction with Dox (upper panel). The IP efficiency was controlled by staining with an anti-ORF75 antibody (middle panel) and the *O*-GlcNAc status of ORF75 was determined by staining with an anti-*O*-GlcNAc antibody (lower panel).

Proteins involved in DNA synthesis and replication are O-GlcNAcylated

Finally, to elucidate the major *O*-GlcNAc-regulated processes in the viral life cycle, functional annotations of all KSHV-encoded proteins were analyzed in relation to the *O*-GlcNAc status of the respective proteins (Table III). In agreement with the main functions of *O*-GlcNAc in eukaryotic cells, O-GlcNAcylated viral proteins were also involved in the regulation of immune responses, protein assembly, gene expression, cell cycle and signaling. However, the largest fraction of O-GlcNAcylated proteins was involved in the modulation of the viral DNA synthesis and replication (Figure 8). In this group, nearly 50% of the proteins are O-GlcNAcylated; this includes (i) proteins involved in nucleotide metabolism, such as ORF2, ORF21, ORF60 and ORF61, (ii) proteins involved in DNA replication and processing such as the viral polymerase/ORF9, the helicase/ORF44, the terminase/ORF29 and the DNA repair enzyme/ORF54 and (iii) the ori-Lyt binding protein ORF K8. Moreover, all proteins involved in viral DNA replication which are not *O*-GlcNAc modified in our screen precipitate with the anti-*O*-GlcNAc CTD110.6 antibody, indicating that they may potentially interact with O-GlcNAcylated proteins (see ORF6, ORF70, ORF37, ORF40/41, ORF46, ORF56, ORF59 and ORF73 in Table I). Together, these data strongly imply that *O*-GlcNAc plays a fundamental role in the regulation of viral DNA replication.

Discussion

O-GlcNAcylation of viral proteins has been described in few cases (Mullis et al. 1990; Novelli and Boulanger 1991; Whitford and Faulkner 1992; Greis et al. 1994; Medina et al. 1998); however, the implications of *O*-GlcNAc in the viral life cycle have not been revealed. Here, we provided evidence that OGT inhibits the amplification and/or spreading of KSHV in a dose-dependent manner. The observed effects may be due to the inhibition of (i) viral or cellular gene expression, (ii) viral DNA synthesis, (iii) the formation and release of viral particles

Table II. Evaluation of the MS analyses

Sample	Accession number	Evaluation by IP		Evaluation by MS			
		O-GlcNAc detection	*O*-GlcNAc intensity	Score	Sequence coverage (%)	No. of *O*-GlcNAc peptides	Peptide identified by MS (specific site underlined, as far as known)
ORF K3	gi|2246549	Yes	+++	2143	75	2	ATYCGGYVGVQSGDGAYSVSCHNK (S278) YRATYCGGYVGVQSGDGAYSVSCHNK (S278)
ORF K10	gi|139472849	Yes	+++	2485	69	7	QVTQASSFTWR (T225) VHPPTTGQFDPLSPR (T338) VFQPTVLYSAPEPAVNPEVSHLPTELER (S594) VPLVSTYAGDR (T632) TPVSHSGPEKPPSK (T709) PSCYNWSPLAEPPATRPIR TPLWIPWSSGGAPNQGLSHTQGGASATPS AGAPPTPEVAER
ORF K8	gi|4585184	Yes	++	325	37	1	TAPSQSGAPGDEHLPCSL (S92)
ORF44	gi|2246487	Yes	++	898	49	1	VAISFGNHR (S727)
ORF21	gi|139472869	Yes	+	2455	75	1	TSYIYDVPTVPTSKPWHLMHDNSLYATPR (S62)
ORF29	gi|139472824	Yes	+	1043	55	1	HHPATPTSANPDVGTPR

IP, immunoprecipitation; +, weak; ++, intermediate; +++, strong. The number in brackets indicates the specific *O*-GlcNAc-modified amino acid residue.

or (iv) the infectivity of newly produced virions. In order to estimate what the major effect may be, we evaluated all KSHV-encoded proteins for *O*-GlcNAc modification using a tripartite IP procedure. To exclude false-positive results, we established a stringent threshold, based on (i) a confirmed *O*-GlcNAc status in three different IP procedures, (ii) the exclusion of protein modification with *N*-linked glycans and (iii) the competition of the *O*-GlcNAc signal with free GlcNAc.

In total, 18 proteins were shown to be *O*-GlcNAc modified, corresponding to 21% of all KSHV-encoded proteins. This coincides with the percentage of *O*-GlcNAc-modified cellular proteins deduced from a bioinformatics study on *O*-GlcNAc site prediction, where 27% (1500 of 5500) of the analyzed human proteins appeared to be *O*-GlcNAcylated (Gupta and Brunak 2002). The *O*-GlcNAc modification of six selected proteins was subsequently verified by nano-LC-ESI-MS/MS. A clear correlation between the number of *O*-GlcNAc peptides and the *O*-GlcNAc intensity in IP could be observed, which confirmed the IP results.

In a recent study, the viral trans-activator ORF50 was identified to be O-GlcNAcylated (Ko et al. 2012). We could confirm the reported results detecting O-GlcNAcylation of ORF50 by IP with the *O*-GlcNAc antibody. However, we could not confirm the O-GlcNAcylation of ORF50 by western blot after IP with the anti-myc antibody. According to our stringent scoring strategy, ORF50 was not among the 18 major O-GlcNAcylated proteins in our study. However, this does not exclude that ORF50 is weakly O-GlcNAcylated, which may be below the detection limit of the *O*-GlcNAc western blot using myc precipitated proteins. Thus, among the 67 proteins not determined to be O-GlcNAcylated in our study, some weak *O*-GlcNAc-modified proteins might still reside.

In this study, out of the 19 KSHV proteins involved in the viral DNA synthesis and replication, 9 were O-GlcNAcylated, namely ORF9, ORF2, ORF21, ORF29, ORF44, ORF K8, ORF54, ORF60 and ORF61. Moreover, from the 10 remaining proteins, 9 appear to interact with O-GlcNAcylated proteins, as they co-precipitate with the anti-*O*-GlcNAc antibody. This indicates that *O*-GlcNAc modification may modulate the viral life cycle by regulating viral DNA replication. Thus, our study adds a new aspect to the possible implications of *O*-GlcNAc modification in the viral life cycle.

However, *O*-GlcNAc modification also affects the regulation of cellular DNA replication, as indicated by previous reports. First, it has been shown that the *O*-GlcNAc level is modulated throughout the cell cycle and the expression of OGT peaks at the M phase (Yang et al. 2012), during which DNA replication is completed and chromosomes are strongly condensed. Second, a pharmacologically induced decrease in *O*-GlcNAc levels leads to a faster progression through the S phase, while increased *O*-GlcNAc levels leads to a cell cycle delay (Slawson et al. 2005). Third, *O*-GlcNAc has been identified on many DNA-binding proteins, such as topoisomerases, DNA repair enzymes and minichromosome maintenance protein (Noach et al. 2007; Zachara et al. 2011; Drougat et al. 2012), indicating that *O*-GlcNAc might play a stabilizing role in DNA repair mechanisms and in the initiation of DNA replication. Finally, the *O*-GlcNAc modification of histone proteins and chromatin remodeling factors has been described previously (Yang et al. 2002; Sakabe et al. 2010), suggesting that *O*-GlcNAc is involved in the organization of the DNA architecture. Together with our data, this implies that the regulation of DNA replication by *O*-GlcNAc might not only be restricted to viruses, but might also occur in eukaryotic cells.

The inhibition of the viral and cellular DNA replication by *O*-GlcNAc results in two protective effects for the infected host: first, increased *O*-GlcNAc abrogates the replication of DNA viruses (e.g. herpesvrisuses) and potentially of certain RNA viruses, which are running through a double-stranded DNA intermediate into their replication process (e.g. retroviruses; Jochmann et al. 2009). Second, increased *O*-GlcNAc may block the proliferation of the infected host cell, resulting

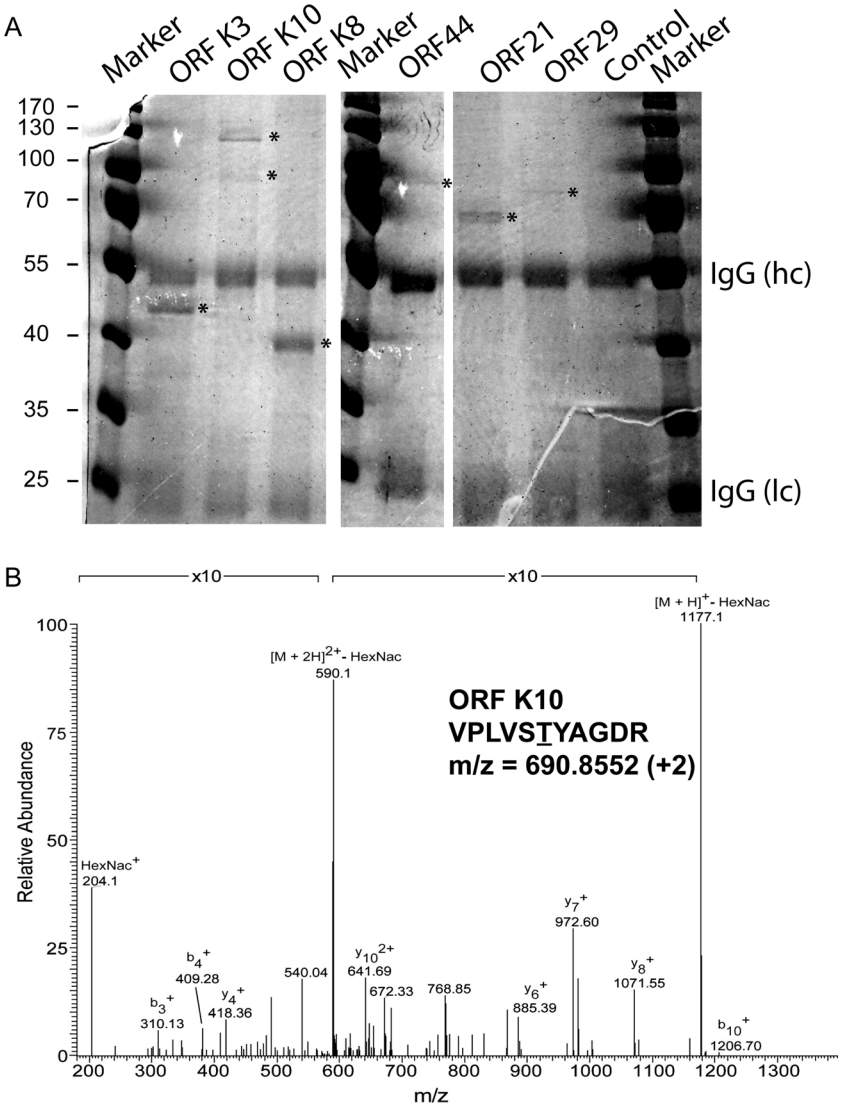

Fig. 7. (**A**) Coomassie staining of immunoprecipitated proteins. A fraction of immunoprecipitates using anti-myc agarose was separated using 10% SDS–PAGE. The enriched proteins were visualized after overnight staining with colloidal coomassie brilliant blue CBB G-250. CV, control vector; IgG(hc), immunoglobulin heavy chain; IgG(lc), immunoglobulin light chain. The asterisks mark the isolated proteins. Both bands in the ORF K10 lane were isolated and contained the ORF K10 protein. (**B**) The MS/MS spectrum of a single tryptic peptide (VPLVSTYAGDR) of ORF K10 containing an *O*-GlcNAc modification on threonine is indicated. The *O*-GlcNAc modified threonine is underlined. Diagnostic *O*-GlcNAc neutral loss fragments and the *O*-GlcNAc oxonium ion ($m/z = 204.08$) in the low molecular weight range of the MS/MS spectrum indicates the *O*-GlcNAc modification of the peptide.

again in the inhibition of virus replication, but also, in the case of tumor-inducing viruses, in the inhibition of tumor growth. This is supported by two studies on a small set of paired tissues from breast or thyroid cancers, where increased OGA enzymatic activity and decreased *O*-GlcNAc levels were detected in primary tumor samples when compared with normal tissue samples (Slawson et al. 2001; Krzeslak et al. 2010). However, it should be mentioned that conflicting data are available on the role of *O*-GlcNAc in cancer progression, as other reports demonstrated that increased *O*-GlcNAcylation is a general characteristic of cancer cells (Slawson and Hart 2011).

Targeting viral replication by *O*-GlcNAc-inducing substances such as PUGNAc, 2-deoxy-D-glucose, glucosamine or Thiamet G will also affect signaling processes in non-infected cells and tissues, which will be associated with side effects. Nevertheless, the therapeutic modulation of O-GlcNAcylation may provide an additional option for combination therapy approaches using reduced concentrations of the pharmacological OGA inhibitors together with antiviral compounds such as ganciclovir, which prevents KSHV replication and KS development (Martin et al. 1999; Casper et al. 2008).

Material and methods

Cell culture and transfection

HEK293T, HEK293, HEK293-rKSHV.219 and iSLK-RTA-KSHV.219 cells were cultivated in Dulbecco's modified eagle

Table III. *O*-GlcNAc status of the KSHV-encoded proteins and correlation to their functions and the pathways they are involved in

Protein	*O*-GlcNAc-ylated	Alternative description	Pathway	Reference
ORF K1	n.d.	Signaling molecule; transmembrane glycoprotein	Signaling	Wang et al. (2004)
ORF4	n.d.	Complement control protein	Immune response, signaling	Spiller et al. (2003)
ORF6	n.d.	Major ssDNA binding protein	DNA synthesis and replication, virus structure and assembly	Nicholas et al. (1997), Ozgur et al. (2011), Wu et al. (2001), Zhu et al. (2005)
ORF7	n.d.	Putative DNA processing and transport protein, capsid assembly	DNA synthesis and replication, virus structure and assembly	Deng et al. (2007), Zhu et al. (2005)
ORF8	+	Envelope glycoprotein B (gB)	Virus structure and assembly, signaling	Baghian et al. (2000), Dyson et al. (2010), Pertel et al. (1998), Zhu et al. (2005)
ORF9	+	DNA polymerase	DNA synthesis and replication	Wu et al. (2001)
ORF10	n.d.	Repressor of interferon signaling	Immune response, signaling	Bisson et al. (2009)
ORF11	n.d.	Homologous to EBV LF2	Unknown	Zhu et al. (2005)
ORF K2	n.d.	Viral interleukin-6	Immune response, signaling	Osborne et al. (1999)
ORF2	+	Dihydrofolate reductase; involved in nucleotide metabolism	DNA synthesis and replication	Cinquina et al. (2000)
ORF K3	+	Modulator of immune recognition-1; transmembrane protein	Immune response, signaling	Coscoy and Ganem (2000), Ishido et al. (2000)
ORF70	n.d.	Thymidylate synthase; enzyme involved in nucleotide metabolism	DNA synthesis and replication	Rose et al. (2003)
ORF K4	n.d.	Viral macrophage inflammatory protein-II	Immune response, signaling	Nakano et al. (2003)
ORF K4.1	n.d.	Viral macrophage inflammatory protein-III	Immune response, signaling	Nakano et al. (2003)
ORF K4.2	n.d.		Unknown	
ORF K5	n.d.	Modulator of immune recognition-2; transmembrane protein	Immune response, signaling	Coscoy and Ganem (2000), Ishido et al. (2000), Sanchez et al. (2002)
ORF K6	n.d.	Viral macrophage inflammatory protein-1	Immune response, signaling	Nakano et al. (2003)
ORF K7	n.d.	Viral inhibitor of apoptosis	Cell cycle and cell death, signaling	Feng et al. (2002), Wang et al. (2002)
ORF16	n.d.	Viral B-cell lymphoma 2	Cell cycle and cell death, signaling	Ojala et al. (2000)
ORF17	+	Protease/capsid assembly protein, scaffolding	Virus structure and assembly	Nealon et al. (2001), Unal et al. (1997), Zhu et al. (2005)
ORF18	n.d.	HVS and MHV-68 homolog	Unknown	Arumugaswami et al. (2006)
ORF19	n.d.	Capsid protein, putative packaging protein	Virus structure and assembly	O'Connor and Kedes (2006)
ORF20	n.d.	Inducer of cell cycle arrest and apoptosis	Cell cycle and cell death, signaling	Nascimento et al. (2009)
ORF21	+	Thymidine kinase; enzyme involved in nucleotide metabolism	DNA synthesis and replication	Gustafson et al. (2000)
ORF22	n.d.	Envelope glycoprotein H (gH)	Virus structure and assembly, signaling	Naranatt et al. (2002), Zhu et al. (2005)
ORF23	n.d.	HVS homolog; tegument protein	Unknown	O'Connor and Kedes (2006)
ORF24	n.d.	MHV-68 homolog; putative tegument protein	Unknown	Bechtel et al. (2005)
ORF25	+	Major capsid protein	Virus structure and assembly	Nealon et al. (2001), Zhu et al. (2005)
ORF26	n.d.	Capsid protein, triplex-2	Virus structure and assembly	Nealon et al. (2001), Perkins et al. (2008), Zhu et al. (2005)
ORF27	n.d.	MHV-68 homolog	Unknown	Zhu et al. (2005)
ORF28	n.d.	Envelope glycoprotein	Virus structure and assembly	Zhu et al. (2005)
ORF29	+	Putative ATPase subunit of terminase, DNA packaging	Virus structure and assembly, DNA synthesis and replication	Deng et al. (2007)
ORF30	n.d.	MHV-68 homolog; putative transcription factor	Gene expression	Wu et al. (2009)
ORF31	n.d.	MHV-68 homolog; putative transcription factor	Gene expression	Jia et al. (2004)
ORF32	n.d.		Unknown	
ORF33	n.d.	Tegument protein involved in viral morphogenesis and egress	Virus structure and assembly	Guo et al. (2009), Zhu et al. (2005)
ORF34	n.d.	MHV-68 homolog; putative transcription factor	Gene expression	Wu et al. (2009)
ORF35	n.d.		Unknown	
ORF36	n.d.	Serine-threonine protein kinase; tegument protein	Signaling	Hamza et al. (2004), Park et al. (2000)
ORF37	n.d.	Alkaline DNA-exonuclease shutoff and exonuclease (SOX)	DNA synthesis and replication, gene expression	Glaunsinger et al. (2005)
ORF38	n.d.	MHV-68 homolog; tegument protein	Unknown	O'Connor and Kedes (2006)
ORF39	n.d.	Envelope glycoprotein M (gM)	Virus structure and assembly	Zhu et al. (2005)
ORF40/41	n.d.	Primase-associated factor	DNA synthesis and replication	Wu et al. (2001)
ORF42	n.d.	HVS homolog; tegument protein	Unknown	O'Connor and Kedes (2006)
ORF43	n.d.	Capsid protein, putative portal protein	Virus structure and assembly	O'Connor and Kedes (2006)
ORF44	+	DNA replication protein (helicase/primase subunit)	DNA synthesis and replication	Wu et al. (2001)
ORF45	n.d.	IRF-7 binding protein	Immune response, signaling	Zhu et al. (2002), Zhu et al. (2010)
ORF46	n.d.	Uracil DNA glucosylase	DNA synthesis and replication	Wang, Chang et al. (2012)
ORF47	n.d.	Envelope glycoprotein L (gL)	Virus structure and assembly, signaling	Naranatt et al. (2002), Zhu et al. (2005)
ORF48	n.d.		Unknown	

Continued

Table III. (Continued)

Protein	*O*-GlcNAc-ylated	Alternative description	Pathway	Reference
ORF49	n.d.	Tegument protein, activates transcription through c-Jun	Signaling	Gonzalez et al. (2006), O'Connor and Kedes (2006)
ORF50	n.d.	RTA	Gene expression	Lukac et al. (1998)
ORF K8	+	Basic-Leucine Zipper/replication-associated protein (K-bZIP/RAP) and ori-Lyt binding protein	Gene expression, DNA synthesis and replication	Wu et al. (2001)
ORF K8.1beta	n.d.	Envelope glycoprotein (gp35-37)	Virus structure and assembly, signaling	Li et al. (1999)
ORF52	n.d.	HVS homolog; tegument protein	Unknown	O'Connor and Kedes (2006)
ORF53	n.d.	Envelope glycoprotein N (gN)	Virus structure and assembly, signaling	Zhu et al. (2005)
ORF54	+	dUTPase; DNA repair	DNA synthesis and replication	Kremmer et al. (1999)
ORF55	n.d.		Unknown	
ORF56	n.d.	Primase	DNA synthesis and replication	Wu et al. (2001)
ORF57	n.d.	Transcriptional and post-transcriptional regulatory protein	Gene expression, DNA synthesis and replication	Han and Swaminathan (2006), Wu et al. (2001)
ORF K9	n.d.	Viral interferon regulatory factor (vIRF)-1	Gene expression, immune response	Gao et al. (1997), Lagos et al. (2007), Seo et al. (2005), Seo et al. (2001), Zimring et al. (1998)
ORF K10	+	vIRF-4	Gene expression, immune response, cell cycle and cell death	Heinzelmann et al. (2010), Lee et al. (2009), Xi et al. (2012)
ORF K10.5	n.d.	vIRF-3, latency-associated nuclear antigen-2 (LANA-2)	Gene expression, immune response	Baresova et al. (2012), Lubyova et al. (2004), Wies et al. (2009)
ORF K11	+	vIRF-2	Gene expression, immune response	Mutocheluh et al. (2011)
ORF58	n.d.	Putative multiple transmembrane protein	Signaling	Gill et al. (2008), May et al. (2005)
ORF59	n.d.	DNA polymerase processivity factor (PF-8)	DNA synthesis and replication	Lin et al. (1998), Wu et al. (2001)
ORF60	+	Ribonucleotide reductase small subunit homolog; enzyme involved in nucleotide metabolism	DNA synthesis and replication	Russo et al. (1996)
ORF61	+	Ribonucleotide reductase large subunit homolog; enzyme involved in nucleotide metabolism	DNA synthesis and replication	Russo et al. (1996)
ORF62	n.d.	Capsid protein, triplex-1	Virus structure and assembly	Nealon et al. (2001), Perkins et al. (2008), Zhu et al. (2005)
ORF63	+	NLRP1 homolog	Immune response	Gregory et al. (2011)
ORF64	n.d.	Deubiquitinase	Signaling	González et al. (2009)
ORF65	n.d.	Small capsid protein	Virus structure and assembly	Nealon et al. (2001), Perkins et al. (2008), Zhu et al. (2005)
ORF66	n.d.		Unknown	
ORF67	n.d.	Viral nuclear membrane-associated protein	Virus structure and assembly	Santarelli et al. (2008)
ORF67.5	n.d.		Unknown	
ORF68	n.d.	Major envelope glycoprotein	Virus structure and assembly	Zhu et al. (2005)
ORF69	+	Viral nuclear membrane-associated protein	Virus structure and assembly	Santarelli et al. (2008)
ORF K12	n.d.	Kaposin	Signaling	Kliche et al. (2001), Li et al. (2002)
ORF K13	n.d.	FLICE-inhibitory protein cellular homolog (vFLIP)	Signaling, cell cycle and cell death	Field et al. (2003), Liu et al. (2002), Thurau et al. (2008)
ORF72	n.d.	Viral cyclin	Signaling, cell cycle and cell death	Chang et al. (1996), Li et al. (1997)
ORF73	n.d.	Latency-associated nuclear antigen -1 (LANA-1)	Gene expression, DNA synthesis and replication	Ballestas et al. (1999), Hyun et al. (2001), Krithivas et al. (2000), Renne et al. (2001)
ORF K14	n.d.	OX-2 membrane-glycoprotein homolog (vOX-2)	Signaling	Chung et al. (2002)
ORF74	n.d.	Viral G protein coupled receptor (vGPCR)	Signaling, gene expression	Bais et al. (1998), Chiou et al. (2002), Pati et al. (2001)
ORF75	+	FGARAT homolog, tegument protein	Signaling	Konrad et al. (2009), Russo et al. (1996), Zhu et al. (2005)
ORF K15	n.d.	Latency-associated membrane protein	Signaling, cell cycle and cell death	Brinkmann et al. (2003), Choi et al. (2000), Sharp et al. (2002)

n.d., not determinable; NLRP1, nucleotide binding and oligomerization, leucine-rich repeat protein-1; FGARAT, formylglycinamide ribotide amidotransferase; EBV, Epstein Barr virus; MHV-68, murine gammaherpesvirus-68; HVS, herpesvirus saimiri; vIRF, viral interferon regulatory factor; FLICE, FADD (Fas-associated protein with death domain)-like interleukin-1 beta-converting enzyme.

medium (PAA, Cölbe, Germany) supplemented with 10% fetal calf serum (FCS; Biochrom, Berlin, Germany) and 2 mM L-glutamine (PAA) at 37°C under 8.5% CO_2. HEK293-rKSHV.219 cells were additionally cultivated with 1 µg/mL puromycin, whereas iSLK-RTA-KSHV.219 cells were additionally cultivated with 1 µg/mL puromycin, 250 µg/mL hygromycin and 250 µg/mL G418 for the continuous selection of infected cells. HEK293T, HEK293 and iSLK-RTA-KSHV.219 cells were authenticated by the German Collection of Microorganisms and Cell Cultures (Braunschweig, Germany) by short tandem-repeat analysis as HEK293T, HEK293 and Caki-1 cell lines, respectively (Stürzl et al. 2013). All cells were routinely tested for

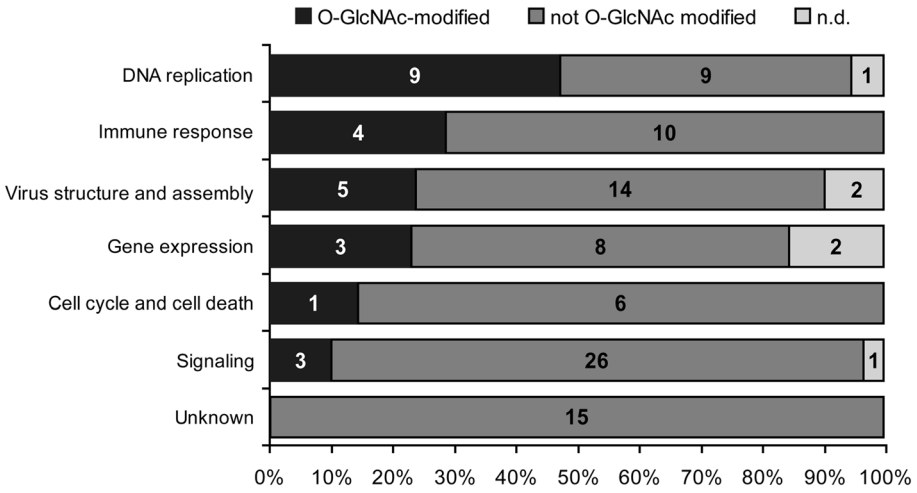

Fig. 8. All 85 KSHV-encoded proteins were sorted according to the published knowledge on their role in the virus life cycle (Table III). The following categories were made: viral DNA synthesis and replication (DNA replication), immune response, virus structure and assembly, gene expression, cell cycle and cell death, signaling and proteins with yet unknown function. Proteins which have been shown to exert more than one function were included in all of the respective groups. The sum of all proteins in a group was set to 100% and the relative amount of *O*-GlcNAc modified, unmodified and not determinable (n.d.) proteins was calculated in percent and is shown.

mycoplasma contamination and were mycoplasma negative. For IP, HEK293T cells were transfected via the calcium phosphate method with plasmids expressing OGT and one of the KSHV-encoded proteins (e.g. pcDNA4-ORF K1, pcDNA4-ORF4 etc.), harvested 2 days after transfection by trypsin/ ethylenediaminetetraacetic acid (EDTA; PAA) and lysed in IP lysis buffer [20 mM Tris–HCl, pH 7.5, 150 mM NaCl, 5 mM $MgCl_2$ and 1% IGEPAL (all purchased from Sigma-Aldrich, Munich, Germany)] supplemented with EDTA-free protease inhibitor cocktail (Roche, Penzberg, Germany). Cell lysates were subjected to IP and western blot analysis. For KSHV replication analysis, HEK293-rKSHV.219 cells were transfected in duplicates or triplicate with either a control vector, a plasmid encoding OGT or a rOGT containing six silent mutations in the siRNA binding site, along with an anti-OGT siRNA (hsOGT_7 SI02665131; Qiagen, Hilden, Germany) depleting OGT. As an alternative, the cells were treated with Thiamet G (#SML0244, Sigma-Aldrich) at the indicated concentrations. In order to induce lytic replication, cells were either transfected with 1 µg pcDNA4-ORF50 (instead of 1 µg control vector) or treated with 3 mM NaBu. Four days post-transfection, the supernatants were collected and used to newly infect HEK293 cells. The remaining HEK293-rKSHV.219 cells were harvested by trypsin/EDTA and counted using a cell counter, lysed in radio immunoprecipitation assay buffer [50 mM Tris–HCl, pH 7.5, 150 mM NaCl, 1% IGEPAL, 0.5% sodium desoxycholate, 0.1% sodium dodecyl sulphate (all purchased for Sigma-Aldrich)] supplemented with EDTA-free protease inhibitor cocktail and subjected to western blot analysis.

KSHV infection of HEK293 cells

HEK293 cells were seeded 24 h prior to infection. On the day of infection, supernatants were collected and cell debris were removed by two times centrifugation at 500 × *g* for 5 min. HEK293 cells were cultivated for 24 h with the virus-containing supernatants prior to media change. After an additional 2 days, the amount of KSHV-infected cells (GFP-positive) was determined by flow cytometry.

Flow cytometry analyses

HEK293 cells infected with the recombinant virus rKSHV.219 were harvested by trypsin/EDTA (PAA), washed twice with fluorescence-activated cell sorting (FACS)-phosphate-buffered saline (PBS) [PBS containing 5% FCS and 0.1% sodium azide (Sigma-Aldrich)] and resuspended in FACS-PBS. A total of 1×10^5 viable cells were analyzed for GFP expression for each sample using a FACSCalibur flow cytometer with CellQuest Pro software (both BD Biosciences, Heidelberg, Germany). The KSHV replication efficiency in the indicator cells infected with the supernatant from producer cells which were either transfected with control vector or mock treated was defined as 100%.

Statistical analyses

Statistical significances were calculated with the Student's *t*-test for paired samples using the SPSS 19.0 software for Microsoft Windows (SPSS Inc., Chicago, IL). All *P*-values smaller than 0.05 were considered statistically significant (*), those smaller than 0.01 highly significant (**) and those smaller than 0.001 highest significant (***).

Data set

Analyses described in this paper were derived on a set of KSHV-encoded genes from a KSHV gene bank library described previously (Sander et al. 2008; Konrad et al. 2009). The sequences consist of 85 well-annotated proteins according to the sequence AF148805 (Glenn et al. 1999). All proteins are expressed within the pcDNA4 plasmid and contain a C-terminal myc tag, except for ORF73/latency-associated nuclear antigen (LANA)-1, which was cloned into the plasmid pcDNA3 without a tag.

Immunoprecipitation

The protein concentration was determined in a microplate reader using a detergent compatible protein assay kit (Bio-Rad, Munich, Germany) according to the manufacturer's protocol. A total of 1 mg protein in a maximal volume of 1 mL was used for the IP. Pre-cleared cell lysates were incubated with the respective antibody-bead complex at 4°C overnight: (i) the anti-*O*-GlcNAc antibody coupled to anti-mouse immunoglobulin M (IgM) (μ-chain specific)-agarose beads, (ii) the anti-myc antibody covalently coupled to agarose beads (Sigma-Aldrich), (iii) the anti-myc antibody coupled to Dynabeads Protein G magnetic beads (Invitrogen) or (iv) the anti-ORF75 antibody coupled to Protein A/G sepharose. On the following day, the beads–coupled protein complexes were washed and either subjected to PNGase F digest or resuspended in 2× Laemmli buffer, denatured at 99°C for 5 min and analyzed by SDS–PAGE and western blot.

PNGase F digest

IP eluates were subjected to PNGase F (cloned from *Flavobacterium meningosepticum* and expressed in *Escherichia coli*, Roche) digest following the manufacturer's instructions. Seven units of PNGase F were used per reaction and incubated for 3.5 h at 37°C. Finally, samples were resuspended in 2× Laemmli buffer, denatured at 99°C for 5 min and analyzed by SDS–PAGE and western blot. As a control, recombinant ovalbumin (#A2512, Sigma-Aldrich) was treated with PNGase F, loaded on SDS–PAGE followed by a silver staining (#PROTSIL2, Sigma-Aldrich) to monitor loading and changes in the molecular weight due to the removal of N-glycosylation. Western blotting of the samples and subsequent staining with the ConA-FITC (500 μg/mL) served to assess changes in N-glycosylation.

SDS–PAGE and western blot

Cell lysates and IP extracts were loaded on acrylamide gels. The separated proteins were transferred to a polyvinylidene fluoride membrane (Roth, Karlsruhe, Germany). Membranes were stained with anti-myc (either #2276 or #2272 from Cell signaling, Frankfurt am Main, Germany, or #9132 from Abcam, Cambridge, UK, diluted 1:1000), anti-GAPDH antibody (from Millipore, Darmstadt, Germany, diluted 1:30,000), anti-ORF73/LANA-1 (Tebu Bio, Offenbach, Germany, #LN-53, diluted 1:1000), anti-*O*-GlcNAc antibody (CTD110.6, Hiss Diagnostics, Freiburg im Breisgau, Germany, diluted 1:1000) or anti-ORF50 antibody (diluted 1:5000), which was kindly provided by Don Ganem (Lukac et al. 1998) or anti-ORF75 antibody (custom rabbit polyclonal, Pineda Antibody Service, Berlin, Germany, diluted 1:30,000). Competition experiments were performed with free GlcNAc (500 mM, Sigma-Aldrich). Secondary antibodies coupled to horseradish peroxidase were diluted 1:5000 (Dako, Hamburg, Germany) and chemiluminescence was detected according to the manufacturer's protocol (Thermo Scientific, Bonn, Germany).

In-gel digestion of proteins

One fraction of the immunoprecipitated cell lysates was separated on 10% acrylamide/bis-acrylamide gels and protein bands were visualized by colloidal Coomassie blue staining (Roth). Proteins were in-gel-digested using trypsin or chymotrypsin (Roche) as described previously (Shevchenko et al. 1996). For chymotrypsin digests, the ammonium bicarbonate buffer was replaced with 100 mM Tris–HCl, pH 7.8. After digestion, the supernatant was removed and transferred into a new tube. The gel pieces were extracted using 70% acetonitrile (ACN)/30% 0.1% formic acid (FA) (v/v) for 15 min and the supernatant was collected. The pooled supernatants were then lyophilized in a vacuum centrifuge and stored at −20°C. For nano-LC-ESI-MS/MS experiments dried samples were resuspended in 0.1% FA.

Mass spectrometry

Nano-LC-ESI-MS/MS experiments were performed on an ACQUITY nano-UPLC (ultra performance liquid chromatography) system (Waters, Milford, MA, USA) directly coupled to a LTQ-Orbitrap XL hybrid mass spectrometer (Thermo Fisher, Bremen, Germany). Tryptic digests of the samples were concentrated and desalted on a pre-column (2 cm × 180 μm, Symmetry C18, 5 μm particle size, Waters) and separated on a 20 cm × 75 μm BEH 130 C18 reversed phase column (1.7 μm particle size, Waters). Gradient elution was performed from 1% ACN to 40% ACN in 0.1% FA within 90 min. The LTQ-Orbitrap was operated under the control of XCalibur 2.0.7 software. Survey spectra (m/z = 250–2000) were detected in the Orbitrap at a resolution of 60,000 at m/z = 400. Data-dependent tandem MS/MS (MS2) mass spectra were generated for the seven most abundant peptide precursors in the linear ion trap using an isolation width of 2 m/z and 35% normalized collision energy. For all of the measurements using the Orbitrap Detector, internal calibration was performed using the polycyclodimethylsiloxane background ion m/z 445.1200 from ambient air as lock mass (Olsen et al. 2005).

Database search

Mascot 2.3 software (Matrix Science, London, UK) was used for protein identification. Spectra were searched against the NCBI protein sequence database downloaded as FASTA-formatted sequences from ftp://ftp.ncbi.nih.gov/blast/db/FASTA/nr.gz. Search parameters specified Trypsin or chymotrypsin as the cleaving enzyme, allowing for three missed cleavages, a 3 ppm mass tolerance for peptide precursors and 0.6 Da tolerance for fragment ions. Carbamidomethylation of cysteine residues was set as the fixed modification and S,T,Y phosphorylation, methionine oxidation and O-HexNac-glycosylation at S and T were considered as variable modifications. MS/MS spectra derived from the fragmentation of phosphorylated peptides and O-glycopeptides were further inspected manually. Neutral loss signals of phosphoric acid and *N*-acetylglucosamine were used as diagnostic ions for phosphorylation and O-GlcNAcylation, respectively. The *O*-GlcNAc oxonium ion (m/z = 204.08) was used as an additional diagnostic marker for *O*-GlcNAc modification if present in the low molecular weight range of the MS/MS spectra.

Supplementary data

Supplementary data for this article is available online at http://glycob.oxfordjournals.org/.

Funding

This work was supported by grants of the Deutsche Forschungsgemeinschaft (STU 238/6-1, SFB796 and STU317/2-1), the German Federal Ministry of Education and Research (BMBF, Polyprobe-Study) and the German Cancer Aid to MS, by grants of the Interdisciplinary Centre for Clinical Research (IZKF) of the University Medical Center Erlangen to MS and to RJ and by grants of the Erlangen's fund for performance-based start-up funding and promotion of young researchers (ELAN) of the University Medical Center Erlangen to RJ.

Acknowledgements

We thank Mahimaidos Manoharan, Katja Schmidt, Ingrid Mons (Division of Molecular and Experimental Surgery, University of Erlangen-Nuremberg) and Berit Würtz (Core Facility of the Life Science Center, University Hohenheim) for their excellent technical assistance, and Dr Christoph Garlichs (Department of Medicine II, Cardiology and Angiology, University of Erlangen-Nuremberg) for kindly providing the FACSCalibur. The generous support of Werner Hohenberger (Director of the Department of Surgery) is gratefully acknowledged.

Conflict of interest

None declared.

Abbreviations

ACN, acetonitrile; ConA, concanavalin A; CTD, carboxy-terminal domain; EDTA, ethylenediaminetetraacetic acid; FA, formic acid; FACS, fluorescence-activated cell sorting; FCS, fetal calf serum; FITC, fluorescein isothiocyanate; GAPDH, glyceraldehyde 3-phosphate dehydrogenase; GFP, green fluorescent protein; HEK293, human embryonic kidney 293; HIV-1, human immunodeficiency virus type-1; Ig, immunoglobulin; IP, immunoprecipitation; KS, Kaposi's sarcoma; KSHV, Kaposi's sarcoma-associated herpesvirus; LANA, latency-associated nuclear antigen; LC-ESI-MS/MS, liquid chromatography–electrospray ionization tandem mass spectrometry; LTQ, linear trap quadrupole; MS, mass spectrometry; NaBu, sodium butyrate; *O*-GlcNAc, *O*-linked *N*-acetyl-D-glucosamine; OGA, *O*-GlcNAc hexosaminidase; OGT, *O*-GlcNAc transferase; ORF, open reading frame; PBS, phosphate-buffered saline; PNGase F, peptide-*N*(4)-(*N*-acetyl-β-D-glucosaminyl)asparagine amidase F; RNA pol-II, RNA polymerase II; rOGT, OGT rescue mutant; RTA, replication and transcription activator; S, serine; SDS–PAGE, sodium dodecyl sulfate–polyacrylamide gel electrophoresis; T, threonine; Y, tyrosine.

References

Arumugaswami V, Wu T-T, Martinez-Guzman D, Jia Q, Deng H, Reyes N, Sun R. 2006. ORF18 Is a transfactor that is essential for late gene transcription of a gammaherpesvirus. *J Virol*. 80:9730–9740.

Baghian A, Luftig M, Black JB, Meng YX, Pau CP, Voss T, Pellett PE, Kousoulas KG. 2000. Glycoprotein B of human herpesvirus 8 is a component of the virion in a cleaved form composed of amino- and carboxyl-terminal fragments. *Virology*. 269:18–25.

Bais C, Santomasso B, Coso O, Arvanitakis L, Raaka EG, Gutkind JS, Asch AS, Cesarman E, Gershengorn MC, Mesri EA. 1998. G-protein-coupled receptor of Kaposi's sarcoma-associated herpesvirus is a viral oncogene and angiogenesis activator. *Nature*. 391:86–89.

Ballestas ME, Chatis PA, Kaye KM. 1999. Efficient persistence of extrachromosomal KSHV DNA mediated by latency-associated nuclear antigen. *Science*. 284:641–644.

Baresova P, Pitha PM, Lubyova B. 2012. Kaposi sarcoma-associated herpesvirus vIRF-3 protein binds to F-box of Skp2 protein and acts as a regulator of c-Myc protein function and stability. *J Biol Chem*. 287:16199–16208.

Bechtel JT, Winant RC, Ganem D. 2005. Host and viral proteins in the virion of Kaposi's sarcoma-associated herpesvirus. *J Virol*. 79:4952–4964.

Bisson SA, Page A-L, Ganem D. 2009. A Kaposi's sarcoma-associated herpesvirus protein that forms inhibitory complexes with type I interferon receptor subunits, Jak and STAT proteins, and blocks interferon-mediated signal transduction. *J Virol*. 83:5056–5066.

Brinkmann MM, Glenn M, Rainbow L, Kieser A, Henke-Gendo C, Schulz TF. 2003. Activation of mitogen-activated protein kinase and NF-kappaB pathways by a Kaposi's sarcoma-associated herpesvirus K15 membrane protein. *J Virol*. 77:9346–9358.

Butkinaree C, Park K, Hart GW. 2010. O-linked beta-N-acetylglucosamine (O-GlcNAc): Extensive crosstalk with phosphorylation to regulate signaling and transcription in response to nutrients and stress. *Biochim Biophys Acta*. 1800:96–106.

Casper C, Krantz EM, Corey L, Kuntz SR, Wang J, Selke S, Hamilton S, Huang M-L, Wald A. 2008. Valganciclovir for suppression of human herpesvirus–8 peplication: A randomized, double- blind, placebo-controlled, crossover trial. *J Infect Dis*. 198:23–30.

Chang Y, Cesarman E, Pessin MS, Lee F, Culpepper J, Knowles DM, Moore PS. 1994. Identification of herpesvirus-like DNA sequences in AIDS-associated Kaposi's sarcoma. *Science*. 266:1865–1869.

Chang Y, Moore PS, Talbot SJ, Boshoff CH, Zarkowska T, Godden K, Paterson H, Weiss RA, Mittnacht S. 1996. Cyclin encoded by KS herpesvirus. *Nature*. 382:410.

Cheng X, Cole RN, Zaia J, Hart GW. 2000. Alternative O-glycosylation/O-phosphorylation of the murine estrogen receptor beta. *Biochemistry*. 39:11609–11620.

Cheng X, Hart GW. 2001. Alternative O-glycosylation/O-phosphorylation of serine-16 in murine estrogen receptor beta. Post-translational regulation of turnover and transactivation activity. *J Biol Chem*. 276:10570–10575.

Chiou CJ, Poole LJ, Kim PS, Ciufo DM, Cannon JS, ap Rhys CM, Alcendor DJ, Zong JC, Ambinder RF, Hayward GS. 2002. Patterns of gene expression and a transactivation function exhibited by the vGCR (ORF74) chemokine receptor protein of Kaposi's sarcoma-associated herpesvirus. *J Virol*. 76:3421–3439.

Choi JK, Lee BS, Shim SN, Li M, Jung JU. 2000. Identification of the novel K15 gene at the rightmost end of the Kaposi's sarcoma-associated herpesvirus genome. *J Virol*. 74:436–446.

Chou T-Y, Hart GW, Dang CV. 1995. c-Myc is glycosylated at threonine 58, a known phosphorylation site and a mutational hot spot in lymphomas. *J Biol Chem*. 270:18961–18965.

Chung YH, Means RE, Choi JK, Lee BS, Jung JU. 2002. Kaposi's sarcoma-associated herpesvirus OX2 glycoprotein activates myeloid-lineage cells to induce inflammatory cytokine production. *J Virol*. 76:4688–4698.

Cinquina CC, Grogan E, Sun R, Lin S-F, Beardsley GP, Miller G. 2000. Dihydrofolate reductase from Kaposi's sarcomaaAssociated herpesvirus. *Virology*. 268:201–217.

Cole RN, Hart GW. 1999. Glycosylation sites flank phosphorylation sites on synapsin I: O-linked N-acetylglucosamine residues are localized within domains mediating synapsin I interactions. *J Neurochem*. 73:418–428.

Comer FI, Hart GW. 2001. Reciprocity between O-GlcNAc and O-phosphate on the carboxyl terminal domain of RNA polymerase II. *Biochemistry*. 40:7845–7852.

Coscoy L, Ganem D. 2000. Kaposi's sarcoma-associated herpesvirus encodes two proteins that block cell surface display of MHC class I chains by enhancing their endocytosis. *Proc Natl Acad Sci USA*. 97:8051–8056.

Deng B, O'Connor CM, Kedes DH, Zhou ZH. 2007. Direct visualization of the putative portal in the Kaposi's sarcoma-associated herpesvirus capsid by cryoelectron tomography. *J Virol*. 81:3640–3644.

Drougat L, Olivier-Van Stichelen S, Mortuaire M, Foulquier F, Lacoste A-S, Michalski J-C, Lefebvre T, Vercoutter-Edouart A-S. 2012. Characterization of O-GlcNAc cycling and proteomic identification of differentially O-GlcNAcylated proteins during G1/S transition. *Biochim Biophys Acta Gen Subj*. 1820:1839–1848.

Dyson OF, Traylen CM, Akula SM. 2010. Cell Membrane-bound Kaposi's sarcoma-associated herpesvirus-encoded glycoprotein B promotes virus latency by regulating expression of cellular Egr-1. *J Biol Chem*. 285:37491–37502.

Feng P, Park J, Lee BS, Lee SH, Bram RJ, Jung JU. 2002. Kaposi's sarcoma-associated herpesvirus mitochondrial K7 protein targets a cellular calcium-modulating cyclophilin ligand to modulate intracellular calcium concentration and inhibit apoptosis. *J Virol*. 76:11491–11504.

Field N, Low W, Daniels M, Howell S, Daviet L, Boshoff C, Collins M. 2003. KSHV vFLIP binds to IKK-gamma to activate IKK. *J Cell Sci*. 116:3721–3728.

Gao SJ, Boshoff C, Jayachandra S, Weiss RA, Chang Y, Moore PS. 1997. KSHV ORF K9 (vIRF) is an oncogene which inhibits the interferon signaling pathway. *Oncogene*. 15:1979–1985.

Gill MB, Edgar R, May JS, Stevenson PG. 2008. A gamma-herpesvirus glycoprotein complex manipulates actin to promote viral spread. *PLoS One*. 3: e1808.

Glaunsinger B, Chavez L, Ganem D. 2005. The exonuclease and host shutoff functions of the SOX protein of Kaposi's sarcoma-associated herpesvirus are genetically separable. *J Virol*. 79:7396–7401.

Glenn M, Rainbow L, Aurade F, Davison A, Schulz TF. 1999. Identification of a spliced gene from Kaposi's sarcoma-associated herpesvirus encoding a protein with similarities to latent membrane proteins 1 and 2A of Epstein-Barr virus. *J Virol*. 73:6953–6963.

Golks A, Tran TT, Goetschy JF, Guerini D. 2007. Requirement for O-linked N-acetylglucosaminyltransferase in lymphocytes activation. *EMBO J*. 26:4368–4379.

Gonzalez SA, Burrone OR. 1991. Rotavirus NS26 is modified by addition of single O-linked residues of N-acetylglucosamine. *Virology*. 182:8–16.

González CM, Wang L, Damania B. 2009. Kaposi's sarcoma-associated herpesvirus encodes a viral deubiquitinase. *J Virol*. 83:10224–10233.

Gonzalez CM, Wong EL, Bowser BS, Hong GK, Kenney S, Damania B. 2006. Identification and characterization of the Orf49 protein of Kaposi's sarcoma-associated herpesvirus. *J Virol*. 80:3062–3070.

Gregory SM, Davis BK, West JA, Taxman DJ, Matsuzawa S-i, Reed JC, Ting JPY, Damania B. 2011. Discovery of a viral NLR homolog that inhibits the inflammasome. *Science*. 331:330–334.

Greis KD, Gibson W, Hart GW. 1994. Site-specific glycosylation of the human cytomegalovirus tegument basic phosphoprotein (UL32) at serine 921 and serine 952. *J Virol*. 68:8339–8349.

Guo H, Wang L, Peng L, Zhou ZH, Deng H. 2009. Open reading frame 33 of a gammaherpesvirus encodes a tegument protein essential for virion morphogenesis and egress. *J Virol*. 83:10582–10595.

Gupta R, Brunak S. 2002. Prediction of glycosylation across the human proteome and the correlation to protein function. *Pac Symp Biocomput*. 310–322.

Gustafson EA, Schinazi RF, Fingeroth JD. 2000. Human herpesvirus 8 open reading frame 21 is a thymidine and thymidylate kinase of narrow substrate specificity that efficiently phosphorylates zidovudine but not ganciclovir. *J Virol*. 74:684–692.

Hamza MS, Reyes RA, Izumiya Y, Wisdom R, Kung HJ, Luciw PA. 2004. ORF36 protein kinase of Kaposi's sarcoma herpesvirus activates the c-Jun N-terminal kinase signaling pathway. *J Biol Chem*. 279:38325–38330.

Han Z, Swaminathan S. 2006. Kaposi's sarcoma-associated herpesvirus lytic gene ORF57 is essential for infectious virion production. *J Virol*. 80:5251–5260.

Hart GW. 1997. Dynamic O-linked glycosylation of nuclear and cytoskeletal proteins. *Ann Rev Biochem*. 66:315–335.

Heinzelmann K, Scholz BA, Nowak A, Fossum E, Kremmer E, Haas J, Frank R, Kempkes B. 2010. Kaposi's sarcoma-associated herpesvirus viral interferon regulatory factor 4 (vIRF4/K10) is a novel interaction partner of CSL/CBF1, the major downstream effector of Notch signaling. *J Virol*. 84:12255–12264.

Hyun TS, Subramanian C, Cotter MA, 2nd, Thomas RA, Robertson ES. 2001. Latency-associated nuclear antigen encoded by Kaposi's sarcoma-associated herpesvirus interacts with Tat and activates the long terminal repeat of human immunodeficiency virus type 1 in human cells. *J Virol*. 75:8761–8771.

Ishido S, Wang C, Lee BS, Cohen GB, Jung JU. 2000. Downregulation of major histocompatibility complex class I molecules by Kaposi's sarcoma-associated herpesvirus K3 and K5 proteins. *J Virol*. 74:5300–5309.

Isono T. 2011. O-GlcNAc-specific antibody CTD110.6 cross-reacts with N-GlcNAc2-modified proteins induced under glucose deprivation. *PLoS One*. 6:e18959.

Iyer SP, Hart GW. 2003. Dynamic nuclear and cytoplasmic glycosylation: Enzymes of O-GlcNAc cycling. *Biochemistry*. 42:2493–2499.

Jackson SP, Tjian R. 1988. O-glycosylation of eukaryotic transcription factors: Implications for mechanisms of transcriptional regulation. *Cell*. 55:125–133.

Jia Q, Wu TT, Liao HI, Chernishof V, Sun R. 2004. Murine gammaherpesvirus 68 open reading frame 31 is required for viral replication. *J Virol*. 78:6610–6620.

Jochmann R, Thurau M, Jung S, Hofmann C, Naschberger E, Kremmer E, Harrer T, Miller M, Schaft N, Stürzl M. 2009. O-linked N-acetylglucosaminylation of Sp1 inhibits the human immunodeficiency virus type-1 promoter. *J Virol*. 83:3704–3718.

Kamemura K, Hart GW. 2003. Dynamic interplay between O-glycosylation and O-phosphorylation of nucleocytoplasmic proteins: A new paradigm for metabolic control of signal transduction and transcription. *Prog Nucleic Acid Res Mol Biol*. 73:107–136.

Kelly WG, Dahmus ME, Hart GW. 1993. RNA polymerase II is a glycoprotein. Modification of the COOH-terminal domain by O-GlcNAc. *J Biol Chem*. 268:10416–10424.

Kliche S, Nagel W, Kremmer E, Atzler C, Ege A, Knorr T, Koszinowski U, Kolanus W, Haas J. 2001. Signaling by human herpesvirus 8 kaposin A through direct membrane recruitment of cytohesin-1. *Mol Cell*. 7:833–843.

Ko YC, Tsai WH, Wang PW, Wu IL, Lin SY, Chen YL, Chen JY, Lin SF. 2012. Suppressive regulation of KSHV RTA with O-GlcNAcylation. *J Biomed Sci*. 19:12.

Konrad A, Wies E, Thurau M, Marquardt G, Naschberger E, Hentschel S, Jochmann R, Schulz TF, Erfle H, Brors B, et al. 2009. A systems biology approach to identify the combination effects of human herpesvirus 8 genes on NF-kappaB activation. *J Virol*. 83:2563–2574.

Kremmer E, Sommer P, Holzer D, Galetsky SA, Molochkov VA, Gurtsevitch V, Winkelmann C, Lisner R, Niedobitek G, Grasser FA. 1999. Kaposi's sarcoma-associated herpesvirus (human herpesvirus-8) ORF54 encodes a functional dUTPase expressed in the lytic replication cycle. *J Gen Virol*. 80 (Pt 5):1305–1310.

Krithivas A, Young DB, Liao G, Greene D, Hayward SD. 2000. Human herpesvirus 8 LANA interacts with proteins of the mSin3 corepressor complex and negatively regulates Epstein-Barr virus gene expression in dually infected PEL cells. *J Virol*. 74:9637–9645.

Krzeslak A, Pomorski L, Lipinska A. 2010. Elevation of nucleocytoplasmic beta-N-acetylglucosaminidase (O-GlcNAcase) activity in thyroid cancers. *Int J Mol Med*. 25:643–648.

Lagos D, Trotter MW, Vart RJ, Wang HW, Matthews NC, Hansen A, Flore O, Gotch F, Boshoff C. 2007. Kaposi sarcoma herpesvirus-encoded vFLIP and vIRF1 regulate antigen presentation in lymphatic endothelial cells. *Blood*. 109:1550–1558.

Lee HR, Toth Z, Shin YC, Lee JS, Chang H, Gu W, Oh TK, Kim MH, Jung JU. 2009. Kaposi's sarcoma-associated herpesvirus viral interferon regulatory factor 4 targets MDM2 to deregulate the p53 tumor suppressor pathway. *J Virol*. 83:6739–6747.

Li H, Komatsu T, Dezube BJ, Kaye KM. 2002. The Kaposi's sarcoma-associated herpesvirus K12 transcript from a primary effusion lymphoma contains complex repeat elements, is spliced, and initiates from a novel promoter. *J Virol*. 76:11880–11888.

Li M, Lee H, Yoon DW, Albrecht JC, Fleckenstein B, Neipel F, Jung JU. 1997. Kaposi's sarcoma-associated herpesvirus encodes a functional cyclin. *J Virol*. 71:1984–1991.

Li M, MacKey J, Czajak SC, Desrosiers RC, Lackner AA, Jung JU. 1999. Identification and characterization of Kaposi's sarcoma-associated herpesvirus K8.1 virion glycoprotein. *J Virol*. 73:1341–1349.

Lin K, Dai CY, Ricciardi RP. 1998. Cloning and functional analysis of Kaposi's sarcoma-associated herpesvirus DNA polymerase and its processivity factor. *J Virol*. 72:6228–6232.

Liu L, Eby MT, Rathore N, Sinha SK, Kumar A, Chaudhary PM. 2002. The human herpes virus 8-encoded viral FLICE inhibitory protein physically associates with and persistently activates the Ikappa B kinase complex. *J Biol Chem*. 277:13745–13751.

Love DC, Hanover JA. 2005. The Hexosamine signaling pathway: Deciphering the "O-GlcNAc Code". *Sci STKE*. 2005:re13.

Love DC, Krause MW, Hanover JA. 2010. O-GlcNAc cycling: Emerging roles in development and epigenetics. *Semin Cell Dev Biol*. 21:646–654.

Lubyova B, Kellum MJ, Frisancho AJ, Pitha PM. 2004. Kaposi's sarcoma-associated herpesvirus-encoded vIRF-3 stimulates the transcriptional activity of cellular IRF-3 and IRF-7. *J Biol Chem*. 279:7643–7654.

Lukac DM, Renne R, Kirshner JR, Ganem D. 1998. Reactivation of Kaposi's sarcoma-associated herpesvirus infection from latency by expression of the ORF 50 transactivator, a homolog of the EBV R protein. *Virology*. 252:304–312.

Martin DF, Kuppermann BD, Wolitz RA, Palestine AG, Li H, Robinson CA. 1999. Oral ganciclovir for patients with cytomegalovirus retinitis treated with a ganciclovir implant. *N Engl J Med*. 340:1063–1070.

May JS, de Lima BD, Colaco S, Stevenson PG. 2005. Intercellular gamma-herpesvirus dissemination involves co-ordinated intracellular membrane protein transport. *Traffic*. 6:780–793.

Medina L, Grove K, Haltiwanger RS. 1998. SV40 large T antigen is modified with O-linked N-acetylglucosamine but not with other forms of glycosylation. *Glycobiology*. 8:383–391.

Mullis KG, Haltiwanger RS, Hart GW, Marchase RB, Engler JA. 1990. Relative accessibility of N-acetylglucosamine in trimers of the adenovirus types 2 and 5 fiber proteins. *J Virol*. 64:5317–5323.

Mutocheluh M, Hindle L, Areste C, Chanas SA, Butler LM, Lowry K, Shah K, Evans DJ, Blackbourn DJ. 2011. Kaposi's sarcoma-associated herpesvirus viral interferon regulatory factor-2 inhibits type 1 interferon signalling by targeting interferon-stimulated gene factor-3. *J Gen Virol*. 92:2394–2398.

Nakano K, Isegawa Y, Zou P, Tadagaki K, Inagi R, Yamanishi K. 2003. Kaposi's sarcoma-associated herpesvirus (KSHV)-encoded vMIP-I and vMIP-II induce signal transduction and chemotaxis in monocytic cells. *Arch Virol*. 148:871–890.

Naranatt PP, Akula SM, Chandran B. 2002. Characterization of gamma2-human herpesvirus-8 glycoproteins gH and gL. *Arch Virol*. 147:1349–1370.

Nascimento R, Dias JD, Parkhouse RM. 2009. The conserved UL24 family of human alpha, beta and gamma herpesviruses induces cell cycle arrest and inactivation of the cyclinB/cdc2 complex. *Arch Virol*. 154:1143–1149.

Nealon K, Newcomb WW, Pray TR, Craik CS, Brown JC, Kedes DH. 2001. Lytic replication of Kaposi's sarcoma-associated herpesvirus results in the formation of multiple capsid species: Isolation and molecular characterization of A, B, and C capsids from a gammaherpesvirus. *J Virol*. 75:2866–2878.

Nicholas J, Ruvolo V, Zong J, Ciufo D, Guo HG, Reitz MS, Hayward GS. 1997. A single 13-kilobase divergent locus in the Kaposi sarcoma-associated herpesvirus (human herpesvirus 8) genome contains nine open reading frames that are homologous to or related to cellular proteins. *J Virol*. 71:1963–1974.

Noach N, Segev Y, Levi I, Segal S, Priel E. 2007. Modification of topoisomerase I activity by glucose and by O-glcnacylation of the enzyme protein. *Glycobiology*. 17:1357–1364.

Novelli A, Boulanger PA. 1991. Deletion analysis of functional domains in baculovirus-expressed adenovirus type 2 fiber. *Virology*. 185:365–376.

O'Connor CM, Kedes DH. 2006. Mass spectrometric analyses of purified rhesus monkey rhadinovirus reveal 33 virion-associated proteins. *J Virol*. 80:1574–1583.

Ojala PM, Yamamoto K, Castanos-Velez E, Biberfeld P, Korsmeyer SJ, Makela TP. 2000. The apoptotic v-cyclin-CDK6 complex phosphorylates and inactivates Bcl-2. *Nat Cell Biol*. 2:819–825.

Olsen JV, de Godoy LM, Li G, Macek B, Mortensen P, Pesch R, Makarov A, Lange O, Horning S, Mann M. 2005. Parts per million mass accuracy on an Orbitrap mass spectrometer via lock mass injection into a C-trap. *Mol Cell Proteomics*. 4:2010–2021.

Osborne J, Moore PS, Chang Y. 1999. KSHV-encoded viral IL-6 activates multiple human IL-6 signaling pathways. *Hum Immunol*. 60:921–927.

Ozgur S, Damania B, Griffith J. 2011. The Kaposi's sarcoma-associated herpesvirus ORF6 DNA binding protein forms long DNA-free helical protein filaments. *J Struct Biol*. 174:37–43.

Park J, Lee D, Seo T, Chung J, Choe J. 2000. Kaposi's sarcoma-associated herpesvirus (human herpesvirus-8) open reading frame 36 protein is a serine protein kinase. *J Gen Virol*. 81:1067–1071.

Pati S, Cavrois M, Guo HG, Foulke JS, Jr, Kim J, Feldman RA, Reitz M. 2001. Activation of NF-kappaB by the human herpesvirus 8 chemokine receptor ORF74: Evidence for a paracrine model of Kaposi's sarcoma pathogenesis. *J Virol*. 75:8660–8673.

Perkins EM, Anacker D, Davis A, Sankar V, Ambinder RF, Desai P. 2008. Small capsid protein pORF65 is essential for assembly of Kaposi's sarcoma-associated herpesvirus capsids. *J Virol*. 82:7201–7211.

Pertel PE, Spear PG, Longnecker R. 1998. Human herpesvirus-8 glycoprotein B interacts with Epstein-Barr virus (EBV) glycoprotein 110 but fails to complement the infectivity of EBV mutants. *Virology*. 251:402–413.

Ranuncolo SM, Ghosh S, Hanover JA, Hart GW, Lewis BA. 2012. Evidence of the involvement of O-GlcNAc-modified human RNA polymerase II CTD in transcription in vitro and in vivo. *J Biol Chem*. 287:23549–23561.

Renne R, Barry C, Dittmer D, Compitello N, Brown PO, Ganem D. 2001. Modulation of cellular and viral gene expression by the latency-associated nuclear antigen of Kaposi's sarcoma-associated herpesvirus. *J Virol*. 75:458–468.

Roos MD, Su K, Baker JR, Kudlow JE. 1997. O glycosylation of an Sp1-derived peptide blocks known Sp1 protein interactions. *Mol Cell Biol*. 17:6472–6480.

Rose TM, Ryan JT, Schultz ER, Raden BW, Tsai C-C. 2003. Analysis of 4.3 kilobases of divergent locus B of macaque retroperitoneal fibromatosis-associated herpesvirus reveals a close similarity in gene sequence and genome organization to Kaposi's sarcoma associated herpesvirus. *J Virol*. 77:5084–5097.

Russo JJ, Bohenzky RA, Chien MC, Chen J, Yan M, Maddalena D, Parry JP, Peruzzi D, Edelman IS, Chang Y, et al. 1996. Nucleotide sequence of the Kaposi sarcoma-associated herpesvirus (HHV8). *Proc Natl Acad Sci USA*. 93:14862–14867.

Sakabe K, Wang Z, Hart GW. 2010. Beta-N-acetylglucosamine (O-GlcNAc) is part of the histone code. *Proc Natl Acad Sci USA*. 107:19915–19920.

Sanchez DJ, Coscoy L, Ganem D. 2002. Functional organization of MIR2, a novel viral regulator of selective endocytosis. *J Biol Chem*. 277:6124–6130.

Sander G, Konrad A, Thurau M, Wies E, Leubert R, Kremmer E, Dinkel H, Schulz T, Neipel F, Stürzl M. 2008. Intracellular localization map of human herpesvirus 8 proteins. *J Virol*. 82:1908–1922.

Santarelli R, Farina A, Granato M, Gonnella R, Raffa S, Leone L, Bei R, Modesti A, Frati L, Torrisi MR, et al. 2008. Identification and characterization of the product encoded by ORF69 of Kaposi's sarcoma-associated herpesvirus. *J Virol*. 82:4562–4572.

Seo T, Park J, Choe J. 2005. Kaposi's sarcoma-associated herpesvirus viral IFN regulatory factor 1 inhibits transforming growth factor-beta signaling. *Cancer Res*. 65:1738–1747.

Seo T, Park J, Lee D, Hwang SG, Choe J. 2001. Viral interferon regulatory factor 1 of Kaposi's sarcoma-associated herpesvirus binds to p53 and represses p53-dependent transcription and apoptosis. *J Virol*. 75:6193–6198.

Sharp TV, Wang HW, Koumi A, Hollyman D, Endo Y, Ye H, Du MQ, Boshoff C. 2002. K15 protein of Kaposi's sarcoma-associated herpesvirus is latently expressed and binds to HAX-1, a protein with antiapoptotic function. *J Virol*. 76:802–816.

Shevchenko A, Wilm M, Vorm O, Mann M. 1996. Mass spectrometric sequencing of proteins silver-stained polyacrylamide gels. *Anal Chem*. 68:850–858.

Slawson C, Hart GW. 2003. Dynamic interplay between O-GlcNAc and O-phosphate: The sweet side of protein regulation. *Curr Opin Struct Biol*. 13:631–636.

Slawson C, Hart GW. 2011. O-GlcNAc signalling: Implications for cancer cell biology. *Nat Rev Cancer*. 11:678–684.

Slawson C, Pidala J, Potter R. 2001. Increased N-acetyl-beta-glucosaminidase activity in primary breast carcinomas corresponds to a decrease in N-acetylglucosamine containing proteins. *Biochim Biophys Acta*. 1537: 147–157.

Slawson C, Zachara NE, Vosseller K, Cheung WD, Lane MD, Hart GW. 2005. Perturbations in O-linked {beta}-N-acetylglucosamine protein modification cause severe defects in mitotic progression and cytokinesis. *J Biol Chem*. 280:32944–32956.

Spiller OB, Robinson M, O'Donnell E, Milligan S, Morgan BP, Davison AJ, Blackbourn DJ. 2003. Complement regulation by Kaposi's sarcoma-associated herpesvirus ORF4 protein. *J Virol*. 77:592–599.

Stürzl M, Gaus D, Dirks WG, Ganem D, Jochmann R. 2013. Kaposi's sarcoma-derived cell line SLK is not of endothelial origin, but is a contaminant from a known renal carcinoma cell line. *Int J Cancer*. 132:1954–1958.

Thurau M, Marquardt G, Gonin-Laurent N, Weinlander K, Naschberger E, Jochmann R, Alkharsah KR, Schulz TF, Thome M, Neipel F, et al. 2008. The viral inhibitor of apoptosis vFLIP/K13 protects endothelial cells against superoxide-induced cell death. *J Virol*. 83:598–611.

Unal A, Pray TR, Lagunoff M, Pennington MW, Ganem D, Craik CS. 1997. The protease and the assembly protein of Kaposi's sarcoma-associated herpesvirus (human herpesvirus 8). *J Virol*. 71:7030–7038.

Vieira J, O'Hearn PM. 2004. Use of the red fluorescent protein as a marker of Kaposi's sarcoma-associated herpesvirus lytic gene expression. *Virology*. 325:225–240.

Wang SS, Chang PJ, Chen LW, Chen LY, Hung CH, Liou JY, Yen JB. 2012. Positive and negative regulation in the promoter of the ORF46 gene of Kaposi's sarcoma-associated herpesvirus. *Virus Res*. 165:157–169.

Wang S, Huang X, Sun D, Xin X, Pan Q, Peng S, Liang Z, Luo C, Yang Y, Jiang H, et al. 2012. Extensive crosstalk between O-GlcNAcylation and phosphorylation regulates Akt signaling. *PLoS One*. 7:e37427.

Wang HW, Sharp TV, Koumi A, Koentges G, Boshoff C. 2002. Characterization of an anti-apoptotic glycoprotein encoded by Kaposi's sarcoma-associated herpesvirus which resembles a spliced variant of human survivin. *EMBO J*. 21:2602–2615.

Wang Z, Udeshi ND, Slawson C, Compton PD, Sakabe K, Cheung WD, Shabanowitz J, Hunt DF, Hart GW. 2010. Extensive crosstalk between O-GlcNAcylation and phosphorylation regulates cytokinesis. *Science Signaling*. 3:ra2.

Wang L, Wakisaka N, Tomlinson CC, DeWire SM, Krall S, Pagano JS, Damania B. 2004. The Kaposi's sarcoma-associated herpesvirus (KSHV/HHV-8) K1 protein induces expression of angiogenic and invasion factors. *Cancer Res*. 64:2774–2781.

Whitford M, Faulkner P. 1992. A structural polypeptide of the baculovirus *Autographa californica* nuclear polyhedrosis virus contains O-linked N-acetylglucosamine. *J Virol*. 66:3324–3329.

Wies E, Hahn AS, Schmidt K, Viebahn C, Rohland N, Lux A, Schellhorn T, Holzer A, Jung JU, Neipel F. 2009. The Kaposi's sarcoma-associated herpesvirus-encoded vIRF-3 inhibits cellular IRF-5. *J Biol Chem*. 284:8525–8538.

Wu FY, Ahn J-H, Alcendor DJ, Jang W-J, Xiao J, Hayward SD, Hayward GS. 2001. Origin-independent assembly of Kaposi's sarcoma-associated herpesvirus DNA replication compartments in transient cotransfection assays and association with the ORF-K8 protein and cellular PML. *J Virol*. 75:1487–1506.

Wu TT, Park T, Kim H, Tran T, Tong L, Martinez-Guzman D, Reyes N, Deng H, Sun R. 2009. ORF30 and ORF34 are essential for expression of late genes in murine gammaherpesvirus 68. *J Virol*. 83:2265–2273.

Xi X, Persson LM, O'Brien MW, Mohr I, Wilson AC. 2012. Cooperation between viral interferon regulatory factor 4 and RTA to activate a subset of Kaposi's sarcoma-associated herpesvirus lytic promoters. *J Virol*. 86:1021–1033.

Yang YR, Song M, Lee H, Jeon Y, Choi E-J, Jang H-J, Moon HY, Byun H-Y, Kim E-K, Kim DH, et al. 2012. O-GlcNAcase is essential for embryonic development and maintenance of genomic stability. *Aging Cell*. 11:439–448.

Yang X, Zhang F, Kudlow JE. 2002. Recruitment of O-GlcNAc transferase to promoters by corepressor mSin3A: Coupling protein O-GlcNAcylation to transcriptional repression. *Cell*. 110:69–80.

Zachara NE, Hart GW. 2004. O-GlcNAc a sensor of cellular state: The role of nucleocytoplasmic glycosylation in modulating cellular function in response to nutrition and stress. *Biochim Biophys Acta Gen Subj*. 1673:13–28.

Zachara NE, Hart GW. 2006. Cell signaling, the essential role of O-GlcNAc! *Biochim Biophys Acta Mol Cell Biol Lipids*. 1761:599–617.

Zachara NE, Molina H, Wong KY, Pandey A, Hart GW. 2011. The dynamic stress-induced "O-GlcNAc-ome" highlights functions for O-GlcNAc in regulating DNA damage/repair and other cellular pathways. *Amino Acids*. 40:793–808.

Zhu FX, Chong JM, Wu L, Yuan Y. 2005. Virion proteins of Kaposi's sarcoma-associated herpesvirus. *J Virol*. 79:800–811.

Zhu FX, King SM, Smith EJ, Levy DE, Yuan Y. 2002. A Kaposi's sarcoma-associated herpesviral protein inhibits virus-mediated induction of type I interferon by blocking IRF-7 phosphorylation and nuclear accumulation. *Proc Natl Acad Sci USA*. 99:5573–5578.

Zhu FX, Sathish N, Yuan Y. 2010. Antagonism of host antiviral responses by Kaposi's sarcoma-associated herpesvirus tegument protein ORF45. *PLoS One*. 5:e10573.

Zimring JC, Goodbourn S, Offermann MK. 1998. Human herpesvirus 8 encodes an interferon regulatory factor (IRF) homolog that represses IRF-1-mediated transcription. *J Virol*. 72:701–707.